Historical geomorphological adjustments of an Upper Rhine sub-tributary over the two last centuries (Bruche River, France)

Timothée Jautzy, Laurent Schmitt, Gilles Rixhon

Géomorphologie : relief, processus, environnement

vol. 28 - n° 1 | 2022
varia

Historical geomorphological adjustments of an Upper Rhine sub-tributary over the two last centuries (Bruche River, France)

Ajustements géomorphologiques historiques d'un sous-affluent du Rhin Supérieur durant les deux derniers siècles (Bruche, France)

Timothée Jautzy, Laurent Schmitt and Gilles Rixhon

Electronic version
URL: https://journals.openedition.org/geomorphologie/16661
DOI: 10.4000/geomorphologie.16661
ISSN: 1957-777X

Publisher
Groupe français de géomorphologie

Printed version
Date of publication: 15 March 2022
Number of pages: 53-72
ISBN: 978-2-913282-94-0
ISSN: 1266-5304

Electronic reference
Timothée Jautzy, Laurent Schmitt and Gilles Rixhon, "Historical geomorphological adjustments of an Upper Rhine sub-tributary over the two last centuries (Bruche River, France)", *Géomorphologie : relief, processus, environnement* [Online], vol. 28 - n° 1 | 2022, Online since 04 March 2022, connection on 14 February 2023. URL: http://journals.openedition.org/geomorphologie/16661 ; DOI: https://doi.org/10.4000/geomorphologie.16661

revue en ligne : https://journals.openedition.org/geomorphologie/

GÉOMORPHOLOGIE : RELIEF, PROCESSUS, ENVIRONNEMENT
vol. 28, n° 1 (2022), p. 53-72
Mise en ligne le 04 mars 2022 sur journals.openedition.org
https://journals.openedition.org/geomorphologie/16661
DOI:10.4000/geomorphologie.16661

http://edytem.univ-savoie.fr/gfg/

Historical geomorphological adjustments of an Upper Rhine sub-tributary over the two last centuries (Bruche River, France)

Ajustements géomorphologiques historiques d'un sous-affluent du Rhin Supérieur durant les deux derniers siècles (Bruche, France)

Timothée Jautzy [a, b*], Laurent Schmitt [a], Gilles Rixhon [a, c]

[a] Laboratoire Image, Ville, Environnement (LIVE UMR 7362), Université de Strasbourg, CNRS, ENGEES, ZAEU LTER, 3 rue de l'Argonne, 67083 Strasbourg, France.
[b] Université du Québec à Rimouski, Département de biologie, chimie et géographie, 300 Allée des Ursulines, G5L 3A1 Rimouski (Québec), Canada
[c] École Nationale du Génie et de l'Eau et de l'Environnement de Strasbourg (ENGEES), 1 quai Koch, 67070 Strasbourg, France

ABSTRACT

Reconstructing evolutionary trajectories of river systems gives valuable insights into the main drivers (i.e. hydro-climatic versus anthropogenic) of their historical morphodynamics. Understanding past and modern adjustments of hydrosystems is therefore a key for appropriate sustainable management schemes. In this respect, the historical evolution (~150 years) of a 6 km dynamic reach of an Upper Rhine sub-tributary, the Bruche River, is thoroughly studied using a wide array of planimetric and topographic data (ancient maps and longitudinal profile, orthophotos, LiDAR). The primary aim is to precisely quantify the lateral and vertical mobility, taking uncertainties into account. Lateral mobility is studied using a specifically designed indicator, the Aggregated Migration rate Index (AMI), which enables precise assessment of planform changes in $m.yr^{-1}$ on elementary sub-reaches (~100 m). A twofold decrease in mean lateral mobility in the mid-20th century, most probably related to functional channel modifications associated with the installation of an underground pipeline, represents the most striking result. Vertical mobility is analysed through the comparison of diachronic LiDAR data (decadal timescale) and historical archive (secular timescale). From the mid-20th century onwards, an unexpected general aggradation of the riverbed (~0.6 m) has occurred, for which several explanations are discussed (i.e. bank erosion, deforestation, sediment release following weir lowering), though remaining speculative. Overall, our results show that historical geomorphological adjustments are primarily controlled by various anthropogenic factors. As the Bruche hosts one of the highest concentrations of spawning beds of emblematic fish species in the French Upper Rhine, this study lays the foundation for future restoration strategies.

Keywords: *Bruche, Upper Rhine, geomorphological adjustments, anthropogenic impacts, evolutionary trajectory, lateral mobility.*

RÉSUMÉ

Reconstituer les trajectoires évolutives des cours d'eau fournit de précieuses informations sur les principaux facteurs de contrôle (hydro-climatiques ou anthropiques) de leur dynamique historique. La compréhension des ajustements passés et modernes des hydrosystèmes constitue un outil majeur dans l'élaboration de plans de gestion durable appropriés. À cet égard, l'évolution historique (~150 ans) d'un tronçon dynamique de 6 km d'un affluent du Rhin Supérieur, la Bruche, est étudiée en utilisant un large jeu de données planimétriques et topographiques. L'objectif principal est de quantifier précisément la mobilité latérale et verticale, en tenant compte des incertitudes. Un indicateur spécialement conçu, l'indice agrégé de migration (AMI), permet d'évaluer avec précision les changements planimétriques en m/an par sous-tronçons élémentaires (~100 m). Le résultat le plus marquant est la diminution de moitié de la mobilité latérale moyenne au milieu du XX^{e} siècle, très probablement liée à de profondes modifications fonctionnelles du chenal, associées à l'installation d'un pipeline souterrain. La mobilité verticale est analysée en comparant des données LiDAR diachroniques (échelle décennale) et des archives historiques (échelle séculaire). A partir du milieu du XX^{e} siècle, une aggradation générale du lit (~0,6 m) est mesurée, pour laquelle plusieurs explications spéculatives sont discutées (mobilisation des sédiments de berges, déforestation, arasement de seuils). Dans l'ensemble, les résultats montrent que les ajustements géomorphologiques historiques sont principalement contrôlés par divers facteurs anthropiques. La Bruche abritant la plus forte concentration de frayères d'espèces de poissons emblématiques dans la partie française du bassin du Rhin Supérieur, cette étude pose les bases de futures stratégies de restauration.

Mots-clés : *Bruche, Rhin Supérieur, ajustements géomorphologiques, impacts anthropiques, trajectoire évolutive, mobilité latérale.*

ARTICLE INFORMATION
Manuscript received on December 21, 2020
revised version received on July 16, 2021
Definitively accepted on September 15, 2021

*Corresponding author. Tél : +33 (0)3 68 85 09 76 ;
E-mail addresses: timothee.jautzy@live-cnrs.unistra.fr (T. Jautzy)
laurent.schmitt@unistra.fr (L. Schmitt)
gilles.rixhon@live-cnrs.unistra.fr (G. Rixhon)

1. Introduction

Over the last centuries, a vast majority of European rivers, in addition to responding to various hydro-climatic controls, have been extensively impacted, either directly or indirectly, by diverse human actions and activities (Petts, 1984; Schmitt et al., 2007; Arnaud et al., 2019; Baena-Escudero et al., 2019; Gregory, 2019). Dating back from the onset of the 19th century onwards, the latter notably include discharge regulation (Winterbottom, 2000), land use change (Liébault and Piégay, 2002; Marston et al., 2003), sediment mining (Comiti et al., 2011; Ziliani and Surian, 2012), channelization, embankment, levee and dam construction (Arnaud et al., 2019; Mandarino et al., 2019). Morphological responses

of hydrosystems resulting from these perturbations, mostly involving channel narrowing and incision (Brown et al., 2018; Baena-Escudero et al., 2019), have been widely documented by studying geomorphological trajectories of river channels (Bravard, 1989, 2017; Surian et al., 2009; Comiti et al., 2011; Armaş et al., 2013). Although it is still complicated to capture the complete breadth of possible impacts resulting from these human activities, we can now reliably assume that the latter certainly are a major controlling factor, if not the main driver, of these modern lateral and vertical adjustments (Liébault and Piégay, 2002; Salit et al., 2015).

Evolutionary trajectory of channel morphology has been extensively studied over the last few decades worldwide (Gurnell et al., 1994; Hawley et al., 2012; Donovan et al., 2015; Dufour et al., 2015; Lovric and Tosic, 2016) as well as in France (Dépret et al., 2017; Duquesne et al., 2020; Eschbach et al., 2018). Along with the analysis of the fluvial sedimentation history (Notebaert and Verstraeten, 2010; Beauchamp et al., 2017), this is often achieved by the historical approach (Lawler, 1993; Simon et al., 2016). It basically consists in using series of historical planimetric and/or vertical data to extract morphological adjustments over time. Although several authors stressed the need to carefully consider spatial uncertainties (Hughes et al., 2006; Liro, 2015; Lea and Legleiter, 2016), especially in mid-sized river systems as these uncertainties might exceed measured planform changes (Piégay et al., 2005, Jautzy et al., 2020), this approach meaningfully allowed gaining new scientific knowledge. The latter was, in turn, successfully transposed into sustainable river management (Baillie et al., 2011; Biron et al., 2014; Arnaud et al., 2015; Marçal et al., 2017; Eschbach et al., 2018).

Draining the Upper Rhine Graben (easternmost France), the Lower Bruche is a mid-sized alluvial river known to have been both laterally active (Maire, 1966; Payraudeau et al., 2010) and affected by anthropogenic activities in modern history. Located in the Strasbourg sub-urban area, this river raises flooding management issues (Payraudeau et al., 2008; Skupinski et al., 2009), especially in the lowermost reach investigated in this study. Against the twofold background of sustainable river management and current/future climatic change (Gregory, 2019), reconstructing the evolutionary trajectory of the Lower Bruche, particularly focusing on historical lateral and vertical channel adjustments, thus requires specific attention. Importantly, this river reach is a key hydrosystem regarding regional hydroecology. Since the reintroduction of the Atlantic salmon in the Upper Rhine during the 90's, the Lower Bruche, including the studied river reach (Largiader et al., 1996), has recorded the highest concentration of spawning beds of both salmon (*Salmo salar* L. ~400) (Gerlier and Roche, 1998) and lamprey (*Petromyzon marinus* ~300) among all rivers draining the French Upper Rhine Graben. All aforementioned key questions not only stress the need to protect the less affected reaches of the Lower Bruche but also highlight a potential of restorating the lateral mobility in those heavily modified reaches.

In this study, we take advantage of an abundant, wide-ranging geographical and historical dataset owing to the specific geographical position of our study area, alternatively disputed by Germany and France over the last centuries, together with its current location inside a major French sub-urban area. First, we aim at precisely quantifying the historical lateral mobility of a 6 km-long reach of the Lower Bruche over the last two centuries, from two maps and eight orthophotos using a specifically-designed Aggregated Migration rate Index (AMI). Second, we document vertical adjustments on both centennial and decadal scales from a longitudinal profile surveyed during World War II combined to diachronic LiDAR-derived Digital Terrain Models (DTM). Finally, we explore the potential controlling factors of fluvial adjustments in the Lower Bruche based on hydrological time series and field investigations.

2. Study area

2.1. Geological and geomorphological setting of the Bruche catchment

The Bruche is a western sub-tributary of the Upper Rhine, located in the easternmost part of France (Bas-Rhin department; fig. 1A). Within a ~730 km²-large catchment, the total elevation difference of this ~80 km-long river from the source (690 m, Vosges Massif) to its confluence (130 m, Ill River) amounts to 560 m (Schmitt et al., 2007; fig. 1B), resulting in an overall longitudinal gradient averaging 7 ‰. The catchment clearly is bipartite considering its geological and geomorphological characteristics. In the upper section (from the source to Mutzig) (fig. 1B), the main trunk and its tributaries drain a wide variety of Paleozoic and Mesozoic rocks peculiar to the northern half of the Vosges Massif (Maire, 1966). These rock formations primarily are plutonic (*e.g.*, granite), volcanic (*e.g.*, rhyolite), sedimentary (*e.g.*, sandstone) and secondarily metamorphic (*e.g.*, gneiss). The whole valley network is deeply entrenched into the Vosges Massif (up to several hundred metres) and the mean slope of the Upper Bruche amounts to 12 ‰. The channel pattern mostly is straight and meandering (though locally affected by human activities) and the floodplain is relatively narrow but show some local enlargements (Schmitt et al., 2007).

By contrast, the 30 km-long lower section drains the eastern part of the Vosgian foothills and the Upper Rhine alluvial plain. Together with a significant decrease of the slope (2.5 ‰), the channel pattern shifts towards a meandering to wandering river within a well-developed, up to several hundred metres-wide Holocene floodplain (fig. 1C). Completely silted up or partly connected paleo-channels and oxbow lakes occur as well (fig. 1C) (Ertlen and Schneider, 2018). Importantly, the floodplain is slightly incised into Pleistocene alluvial formations. The latter, mostly consisting in a complex juxtaposition of fan deposits and a system of sandy/gravely alluvial terraces, are frequently capped by Holocene loess (Maire, 1966). As for terrace formation, Late Quaternary paleoclimatic fluctuations received much attention (Baulig, 1922; Théobald, 1955; Millot et al., 1957; Castela and Tricart, 1958; Buraczynski and Butrym, 1984; Lautridou et al., 1985). However, Maire (1967) and Vogt (1992) also pointed out the role of neotectonics as the Lower Bruche valley is located in the direct vicinity of a main normal fault system of the Upper Rhine Graben.

2.2. Significant anthropogenic forcing in the Lower Bruche

Although paleoclimatic variations and/or neotectonics surely controlled the Lower Bruche evolution, a growing human influence over the last centuries has played – and still plays – a major role on modern fluvial dynamics. In addition to catchment-wide land cover changes, *e.g.*, deforestation in the Vosgian part during the medieval period (Gebhardt et al., 2015), the ~20 km-long "Canal de la Bruche"

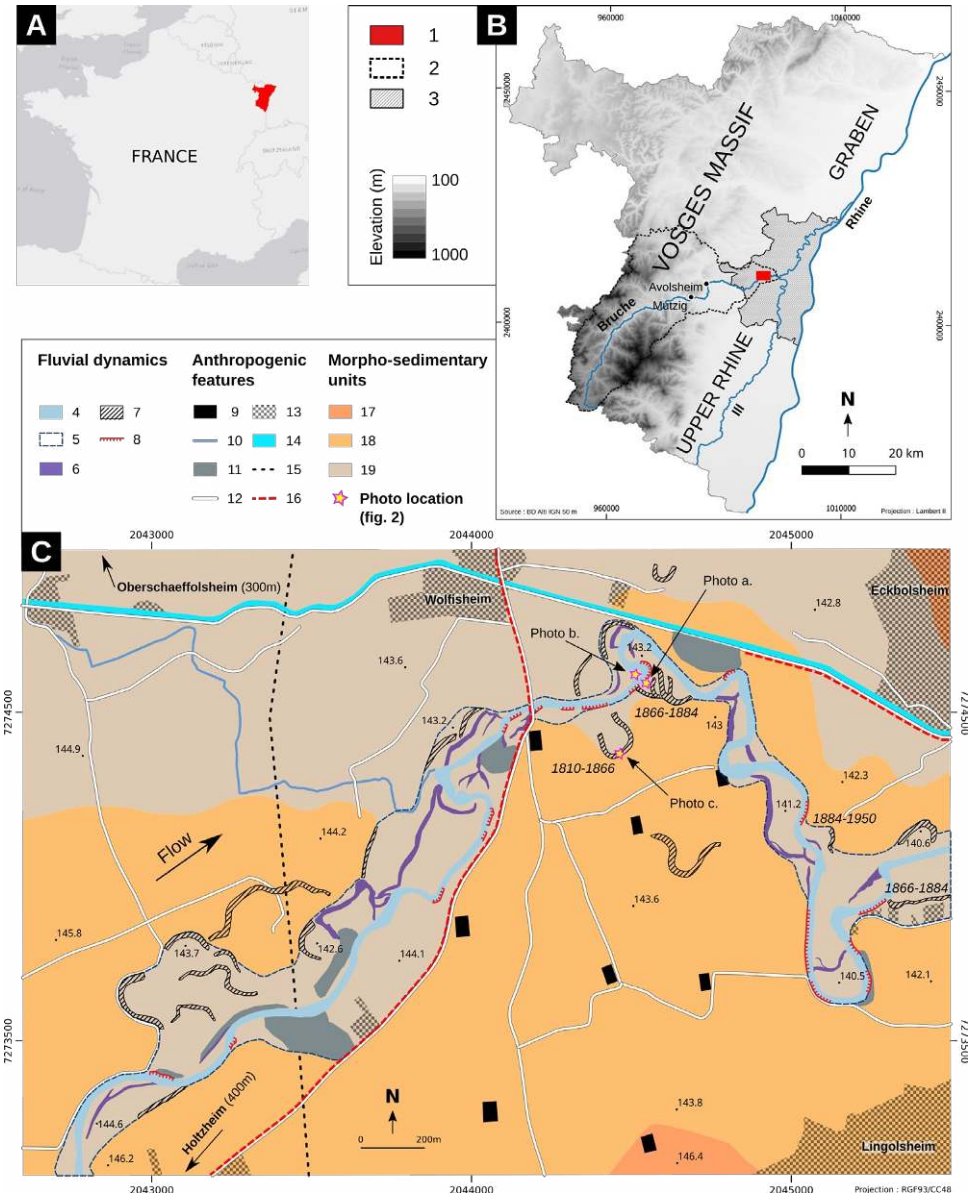

Fig. 1 – Study area.

A: Bas-Rhin department in easternmost France. B: Location of the study reach in the very downstream part of the bipartite Bruche catchment. 1. Studied reach; 2. Bruche catchment; 3. Strasbourg urban area. C: simplified geomorphological map of the six kilometres-long studied reach (partly based on Maire, 1966). 4. Current active channel; 5. Extension of flooding area; 6. Flood channels; 7. Paleochannels, including oxbow lakes (period of abandonment indicated in italics when documented); 8. Active bank erosion; 9. 19th century blockhouse; 10. Irrigation channel; 11. Embankment/artificial filling; 12. Pathways; 13. Villages/residences; 14. Bruche canal; 15. Underground pipeline; 16. High flow dikes; 17. Postulated LGM terrace (Maire, 1966); 18. Postulated post-LGM terrace (Maire, 1966); 19. Holocene floodplain (Maire, 1966).

Fig. 1 – Zone d'étude.

A : département du Bas-Rhin à l'extrémité est de la France. B : Localisation du tronçon étudié à l'extrémité aval du bassin versant bipartite de la Bruche 1. Tronçon étudié ; 2. Bassin versant de la Bruche ; 3. Aire urbaine de Strasbourg. C : carte géomorphologique simplifiée de la zone d'étude (partiellement basé sur Maire, 1966). 4. Lit actif actuel ; 5. Limites de la plaine inondable ; 6. Chenaux de crue ; 7. Paléochenaux (période d'abandon indiquée en italique lorsque documentée) ; 8. Érosion de berges active ; 9. Blockhaus du XIXe s. ; 10. Chenal d'irrigation ; 11. Enrochement/Remblai ; 12. Chemins ; 13. Villages/résidences ; 14. Canal de la Bruche ; 15. Pipeline souterrain ; 16. Digues de hautes eaux ; 17. Terrasse würmienne supposée (Maire, 1966) ; 18. Terrasse post-würmienne supposée (Maire, 1966) ; 19. Plaine alluviale holocène (Maire, 1966).

(fig. 1C) represents one of the first major anthropogenic impact on hydromorphological dynamics of the Lower Bruche (Maire, 1966). Ordered by Louis XIV, its construction led by De Vauban in 1682 aimed at supplying Strasbourg in raw material to build fortifications (Haettel and Haettel, 2012). Partly fed by the Bruche river itself, the up to ten metres-wide canal starts upstream in the locality of Avolsheim (fig. 1B). Until its outlet with the Ill, it roughly follows the river course, either very close to it (5 m) or more remotely (2000 m).

It is unequivocally acknowledged that the river channel itself has been impacted by anthropogenic activities at different levels. Total artificialization (channelization), high, moderate and low rectification approximately represent 24, 16, 30 and 30 % of the whole lower reach (from Mutzig to the confluence), respectively (Maire, 1985). Some of these modifications happened during the industrialization period (broadly from 1850 to 1950), especially for textile and steel production as well as forestry development (Guéry, 1962; Leypold, 1995; Klein, 2005). These activities all took large advantage of the river hydraulic energy. Some irrigation ditches were also excavated in the alluvial foodplain and weirs were constructed across the channel. One of them corresponds to the crossing of an underground pipeline in the study reach, erected in 1965 (Maire, 1966). The Bruche catchment is currently affected by around four hundred levees of different kind (Sandre referential of flow obstacles, *Office Français de la Biodiversité* - OFB). Even after the decline of these industries, rectifications, dike constructions and embankments had been performed until about 2000, mostly related to the growing urbanization of the Lower Bruche area. The main purpose of these modifications has meanwhile shifted from exploiting the river energy to protecting the riverine areas and populations, by constructing high flow dikes (fig. 1C).

2.3. Field survey of the most dynamic reach of the Lower Bruche

This present study focuses on a six kilometres-long wandering reach (fig. 1B). It is comprised between Holtzheim, where the daily two-year (Q2) and ten-year (Q10) peak flow discharges amount to 71 and 126 $m^3.s^{-1}$ (from the gauge station of Holtzheim), respectively, and Eckbolsheim/Lingolsheim where the downstream end is located

2.7 km upstream from the Ill confluence (fig. 1C). The average bankfull width of the active channel amounts to ~20 m. According to Schmitt et al.'s (2007) morphodynamic typology of rivers draining the French part of the Upper Rhine Graben, the studied reach is categorized as a "river with moderate energy and high lateral dynamics". Interestingly, its specific stream power assessed for the Q2 discharge (27 W/m²) falls in the theoretical lower range usually reported in the literature between laterally active and inactive reaches 25–35 W/m² (Brookes, 1987; Orr et al., 2008; Bizzi and Lerner, 2015; Dépret et al., 2017).

This peculiar reach is selected because it has been laterally active over historical times, despite the significant anthropogenic features and impacts presented above (e.g. Bruche canal, irrigation channels, underground pipeline, embankments, roads and pathways) (fig. 1C). In his study along the entire Lower Bruche, Maire (1966) identified a peak of modern fluvial dynamics in this reach. This was later complemented by the study of Payraudeau et al. (2010) highlighting meander migration rates ranging between 0.1 and 2.7 m.yr^{-1} in the same area.

Our preliminary field survey allowed documenting a wide range of processes and associated landforms related to past and present river dynamics. As a comprehensive and detailed description of these obviously is beyond the scope of this study, we thus briefly report here the most relevant observations for the present work. The river develops abundant meanders in the floodplain, whose width ranges from ~100 in the northeastern part to ~400 m in the western part of the studied area. The current river channel also locally erodes the Pleistocene terrace (fig. 1C). Both proximal and distal processes and landforms are recognised in the floodplain and will be subdivided accordingly.

As for the first category, active and sustained retreat of the outer bank characterized by a fining-upward sequence has been recently documented in the most actively migrating meander of the whole reach (Payraudeau et al., 2010). In contrast, ridge-and-swale topography (fig. 2B) along with point bar deposits (fig. 2A) at the tip of the inner bank of the very same meander bear witness of lateral accretionary processes and progressive eastward migration of the whole system. Note that a further shaping of this morphology is achieved through modern flood events (fig. 2B).

As for the second category, numerous flood channels and paleochannel segments occur both in the floodplain (along both river sides) and the lower terrace (fig. 1C). Among paleochannels, we identified well-preserved paleomeanders along with their associated morphology, such as the scarp of a former concave bank scoured in the lower (possibly post-LGM) terrace (fig. 2C). Whilst this observation strongly points to past meander cut-off processes, a stepwise downstream shift of a paleomeander within the floodplain is clearly documented as well.

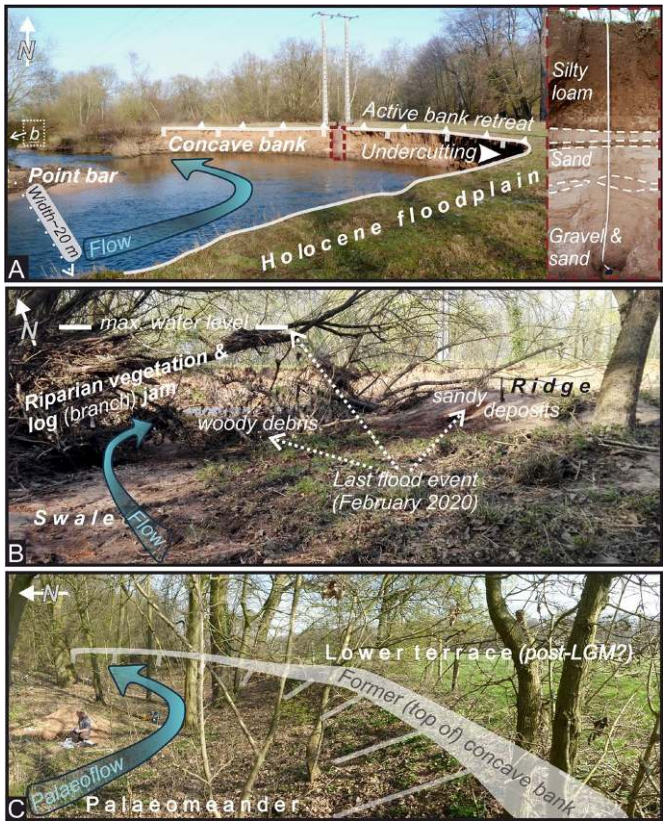

Fig. 2 – Geomorphological processes and correlated landforms in the studied reach of the Lower Bruche.

A: active bank retreat due to bank undercutting favoured by a fining-upward sequence (see right photo) building most of the Holocene floodplain. B: active flooding processes and high-water marks of the 2020 flood event in the opposite inner bank characterised by a ridge-and-swale topography. C: lower terrace eroded by a well-preserved paleomeander belonging to morpho-sedimentary units 18 and 19 in Figure 1C, respectively.

Fig. 2 – Processus géomorphologiques et morphologies associées dans le tronçon étudié de la Basse Bruche.

A : retrait de berge actif entretenu par le granoclassement normal caractérisant les séquences sédimentaires (voir photo de droite) formant la plaine alluviale holocène. B : processus en rive convexe opposée, caractérisée par une succession de bourrelets-gouttières, avec laisses de crue en lien avec le dernier épisode de crue (2020). C : basse terrasse érodée par un paléoméandre, appartenant respectivement aux unités morpho-sédimentaires 18 et 19 de la Figure 1C.

3. Methodology

3.1. Lateral mobility

3.1.1. Data processing and error assessment

To reach a satisfactory balance between quality and availability of remotely sensed data, two ancient maps and eight orthophotos were selected (tab. 1). Following on from this, we excluded an orthophoto of 1932 due to its poor quality, resulting in a significant data gap between 1884 and 1950 (*i.e.*, 66 years). The first and second maps were produced by the French Headquarters (*Etat Major*) in 1866 and the German Military Geographic Institute (*Militärgeographisches Institut*) in 1886, respectively. Our dataset is completed by two diachronic LiDAR-derived DTM, surveyed in 2006 and 2015. Spanning altogether 65 years (from 1950 to 2015), the eight orthophotos and the two DTMs originate from different producers (national, regional and local institutions) and are consequently delivered with various projections and resolutions, ranging from 16 to 50 cm. Orthophotos and DTMs were re-projected in the RGF93/CC48 (EPSG: 3948) coordinate reference system (CRS), which is the most accurate projection system in this area.

In QGIS, both maps were co-registered to the 1950 orthophoto, which is the closest in time, and where some mapped pathways are visible. For the 1866 and 1884 maps, eight and eleven ground control points (GCPs) were used, respectively, resulting in root mean square errors (RMSE) of 3.4 and 4.2 m based on a 2nd degree polynomial transformation. Both soft (pathway intersections) and hard (canal, buildings) features were employed. Owing to the stability of the canal through time, its proximity to the river channel (fig. 1C) was particularly helpful in achieving good coregistrations.

Table 1 – List of planimetric data used in this study and their main characteristics.
Tableau 1 – Liste des données planimétriques utilisées dans cette étude et leurs principales caractéristiques.

Year	Month-Day	Type	Scale/Resolution	Source	Geometric error (source)
1866	/	M	1/40 000	French «Etat Major»	3.4 m (1)
1884	/	M	1/25 000	Germany Military Geographic Institute	4.2 m (1)
1950	9-13	OP	50 cm	IGN	0.87 m (2)
1956	4-10	OP	50 cm	IGN	1.25 m (2)
1964	4-17	OP	20 cm	LIVE	0.94 m (2)
1978	9-17	OP	30 cm	LIVE	1.09 m (2)
1986	6-27	OP	37 cm	EMS	1.06 m (2)
1998	6-21	OP	16 cm	EMS	0.81 m (2)
2006	2-25	LIDAR	100 cm	CG 67	0.5 m (3)
2011	6-27	OP	20 cm	CIGAL	0.47 m (2)
2015	11-8	LIDAR	50 cm	EMS	0.1 m (3)
2015	summer	OP	20 cm	IGN	0 m (reference)

M: map; OP: orthophoto; IGN: French National Geographic Institute; LIVE: Laboratoire Image Ville Environnement; EMS: Strasbourg European Metropolis (Eurométropole de Strasbourg); CG67: Bas-Rhin Department; CIGAL: Cooperation for Geographical Information in Alsace (Coopération pour l'Information Géographique en ALsace). Geometric error values originate from (1) the coregistration RMSE, (2) RMSE calculated from an independent point set and (3) the data producer.

M : carte ; OP : orthophoto ; IGN : Institut Géographique national ; LIVE : Laboratoire Image Ville Environnement ; EMS : Eurométropole de Strasbourg ; CG67 : Conseil Départemental du Bas-Rhin ; CIGAL : Coopération pour l'Information Géographique en ALsace. Les valeurs de l'erreur géométrique proviennent (1) du RMSE de géoréférencement, (2) du RMSE calculé depuis un set de points indépendants et (3) du producteur de données.

The availability of LiDAR-derived DTMs also allowed confirming a satisfactory map coregistration as some paleochannels identified on DTMs corresponded to ancient active channels visible on the co-registered maps.

As for the orthophotos, the geometric error was assessed through an independent set of GCPs (Hughes et al., 2006; Lea and Legleiter, 2016; Jautzy et al., 2020). A total of eighteen points were selected on each orthophoto, among which five hard and thirteen soft features. The spatial distribution of the GCPs was as uniform as possible over the whole study area. The geometric error was calculated by measuring the planimetric difference (RMSE) between the test points set and the reference points (2015). Throughout the study area, the geometric error calculated from the independent GCPs ranges from 0.47 to 1.25 m (tab. 1). The geometric error was not assessed for both maps as the 18 GCPs selected on the orthophotos were unrecognizable. We thus used the coregistration RMSE (tab. 1).

Widely used by fluvial geomorphologists using remotely sensed data, the concept of active channel refers to the unvegetated area (i.e. surfaces of water and unvegetated bars) and allows to objectively delineate bankfull channel boundaries on aerial photographs (Winterbottom, 2000; Liébault and Piégay, 2001; Surian et al., 2009; Liro, 2015; Mandarino et al., 2019). In this study, a single experimented user digitized active channel boundaries in QGIS at a 1/300 scale. Given that procedure and the fact that most of the orthophotos were surveyed during low or moderate flows (tab. 1), which are favourable conditions to strongly reduce the operator digitization error by not including vegetated bars potentially submerged during high flows (Werbylo et al., 2017), we may reasonably assume that the latter was kept very low. Furthermore, to avoid erroneous digitization of active channel contours, one must consider the potential impeding effect of riparian vegetation. Whilst the latter has constantly evolved since the 50's in our study area (Skupinski et al., 2009), the LiDAR-derived DTMs strongly helped in achieving an accurate identification of channel contours (*i.e.,* bank positions) through the removal of this vegetation. We thus assume that the interpretation bias caused by riparian vegetation was very low too (Payraudeau et al., 2010; Werbylo et al., 2017). As for the maps, channel boundaries were digitized just as they are represented on maps.

3.1.2. Quantification of historical lateral adjustments

The channel in the studied reach is prone to be affected by temporal planform changes that not only vary in amplitude but also in type (*i.e.,* natural vs man-made). Since we aim to longitudinally quantify any type of channel changes in an intelligible unit (m/yr), we developed a specifically-designed index called Aggregated Migration rate Index (AMI). It basically refers to the "channel overlay" method (Downward et al., 1994; Gurnell et al., 1994; Yao et al., 2011; Lovric and Tosic, 2016; Jautzy et al., 2020), although it does not distinguish between eroded and deposited surfaces. Merging any kind of planform change into a single metric, AMI actually allows the quantification of lateral mobility in an intelligible unit ($m.yr^{-1}$) between each documented date. Since the studied reach is purely alluvial, *i.e.,* unconfined setting (Schumm, 1985; Brierley and Fryirs, 2013), neither specific topographic criteria nor DTM could be used to determine a reference centerline. Moreover, the historical lateral mobility being relatively high, we chose not to use a particular thalweg as a reference centerline. In our opinion, this would have biased the extraction of migration rates since the position of the thalweg changed considerably.

Thus, the reference centreline has been digitized as the axis of the whole historical lateral mobility space. We subdivided the latter into 38 sub-reaches (fig. 3, 6), orthogonally to the reference centreline, using Fluvial Corridor Toolbox (Roux et al., 2015). The AMI between time t_1 and t_0 can be mathematically expressed as:

$$AMI_{t_1\text{-}t_0} = \frac{channel_{t_1}[m^2] - channel_{t_0}[m^2] + EroDepo[m^2]}{L\,[m] \times (t_1 - t_0)\,[yr]} \quad [1]$$

where ($channel_{t1}$-$channel_{t0}$) corresponds to the new channel surface [m²] , EroDepo to the surface (if any) referred to as "eroded then deposited" comprised between the former channel (t_0) and the new one (t_1) [m²], and *L* to the sub-reach length [m] (fig. 3). Note that the EroDepo surface does not always involve continuous lateral channel migration followed by deposition (Jautzy et al., 2020) but may correspond to channel lateral shifts via meander cut-off for instance. The Figure 3 illustrates how the methodology was implemented along sub-reaches 27 to 32, between 1884 and 1950.

To explore planform changes at the scale of the entire reach, we also assessed the evolution of the active channel width as well as the sinuosity. For each date, the active channel width (*w*) is calculated as a mean value of the entire reach as follows:

$$w = \frac{A}{L} \quad [2]$$

The active channel area (*A*) is extracted from the channel polygons. The thalweg length (*L*) is evaluated as the mean of the two banks length extracted from the channel polygons (Schook et al., 2017). Sinuosity is calculated by dividing the thalweg length (*L*) by the euclidian distance (*D*) between the very upstream and downstream extremities of our reach (Charlton, 2008; Dey, 2014).

$$S = \frac{L}{D} \quad [3]$$

As the latter distance is constant in time, sinuosity evolution actually represents the thalweg length evolution.

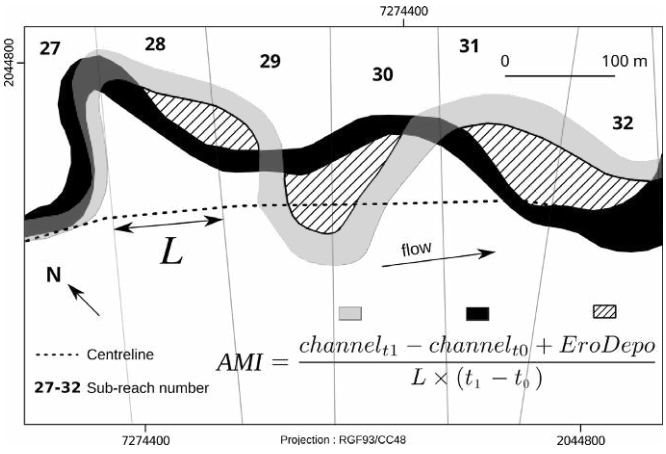

Fig. 3 – Planimetric excerpt illustrating the methodology used to calculate the Aggregated Migration rate Index (AMI).

Fig. 3 – Extrait planimétrique illustrant la méthodologie utilisée pour calculer l'Indice agrégé de migration (AMI).

3.2. Vertical evolution

3.2.1. Data processing

To document the channel bottom elevation evolution, two types of data were used. The first one corresponds to a longitudinal profile (including the thalweg and an unspecified bank) surveyed by the German military geographic institute around 1940 during the occupation in World War II (Volkmann and Müller, 1999; Eckhard Wirbelauer, oral communication). The second one corresponds to the 2006 and 2015 LiDAR points clouds, from which the DTMs presented in table 1 have been extracted. The 2006 cloud is unclassified, has a density of 3.5 points/m², and a vertical and horizontal precision amounting to 15 and 50 cm, respectively. The 2015 cloud is classified and colorized, has a density of 20 points/m², and a 10 cm vertical and horizontal precision.

While the water elevation can be usually assessed by the topo-bathymetric LiDAR (Legleiter, 2012), those used in this study were tuned to capture the relief above the water level. An unrealistic elevation of water surfaces is consequently expected as the latter were interpolated from the basal part of the channel banks on both terrestrial LiDAR-derived DTMs. More generally, even if most LiDAR pulses are absorbed by water, some of them are returned and measured (*e.g.*, orthogonal angle of incidence with water, reflection by floating leaves or in sections of turbulent water surfaces) (fig. 4). By re-analyzing and processing the original 3D point clouds, one can extract the profile of the actual water surface (Magirl et al., 2005; Cavalli et al., 2008; Legleiter, 2012; Biron et al., 2013; Lallias-Tacon et al., 2014; Chen et al., 2017). This can be used in turn as an approximation for the channel bottom profile, referring both to the 2006 and the 2015 points clouds.

3.2.2. Longitudinal profiles extraction and overlay

Using CloudCompare©, we first clipped the point cloud with the corresponding active channel determined on DTMs. The cloud is then converted in a x,y,z layer and exported to QGIS. Points whose elevation cannot correspond to the water surface are deleted, *i.e.,* any point with a z value upper than the one measured at the very upstream of our study reach. We assume the process allowed us to also eliminate most of the riparian vegetation. For the 2015 cloud, vegetation has been removed thanks to the classification. We then manually modified the active channel layer to avoid points corresponding to banks and alluvial bars. For the 2015 cloud, this has been helped by the 2015 orthophoto, captured few months before (tab. 1, fig. 4B). Once we assumed the buffer contained only water points, we disaggregated it in 20 m sections using the Fluvial Corridor Toolbox (Roux et al., 2015). This allows us to calculate the mean water surface elevation per sections from ~75 and ~140 points/sections respectively

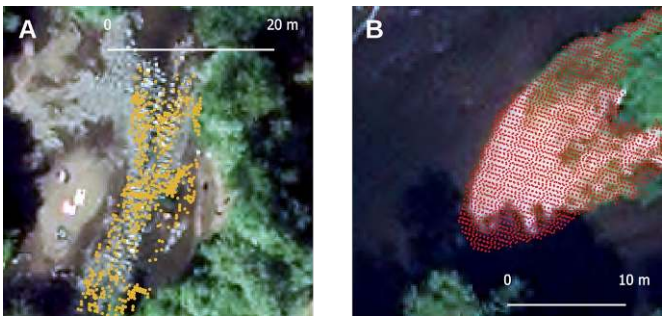

Fig. 4 – Examples of terrestrial LiDAR pulses reflections in an active channel (2015 orthophoto).

A: yellow points represent the water elevation because pulses are reflected on a riffle. B: red points represent the elevation of a mid-channel bar.

Fig. 4 – Exemples de réflexions des pulsations d'un LiDAR terrestre dans un chenal actif (orthophoto 2015).

A : les points jaunes représentent l'altitude réelle de la surface en eau car les pulsations sont réfléchies sur un radier. B : les points rouges représentent l'altitude d'un banc central.

for the 2006 and the 2015 points clouds. Water surface elevation is then converted into channel bottom elevation, by deducting 75 and 40 cm from the 2006 and the 2015 water surface profiles, respectively. These values correspond to the water level gauged at Holtzheim, 1.2 km upstream the study area, the days the LiDARs were surveyed. Our field knowledge of the river's bathymetry allowed confirming that the water depth at the gauging station is of the same order of the one at the study reach, except for riffles and pools which are both very localised. Concerning the German survey (20th), the thalweg and the unspecified bank elevation values were directly measured from the paper document (fig. 5) and reported in a spreadsheet.

To explore the evolution of the unspecified bank elevation from 1940 to nowadays, the longitudinal profiles of both banks (left and right) have been also extracted from the 2015 DTM at 15 m from the contour of the digitized 2015 active channel.

To document channel bottom and bank evolution through time, simultaneous plotting of elevation data from the 20th survey onto those of the 21st survey required both horizontal and vertical corrections. Indeed, the thalweg length decreased by about 200 m between the 1950 and the 2015 orthophoto and the vertical datum used for the document of the 20th century differs from the one used for the LiDAR points clouds. Horizontal corrections were made possible owing to the existing bridges reported on the 20th document, by a manual uniform contraction of the 20th profiles (channel bottom and banks). Vertical corrections consisted in converting elevations to a common vertical datum (EVRF2000), which is based on the Normaal Amsterdams Peil as the zero-level, resulting in a subtraction of 0.486 m from the 21st profile. This value has been provided by the IGN (French National Geographic Institute).

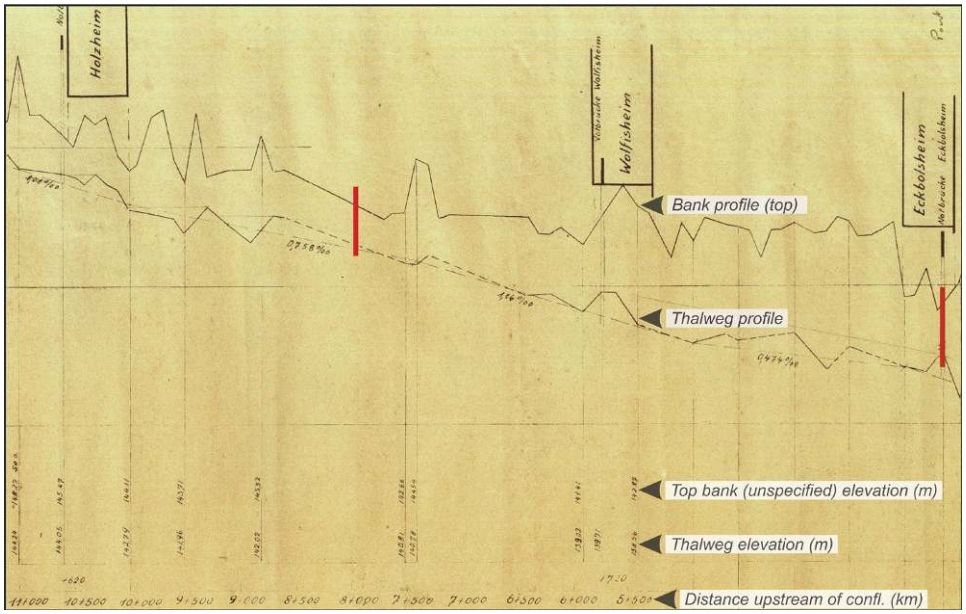

Fig. 5 – Excerpt from the Bruche longitudinal profile along the studied reach (delimited by red marks), surveyed during World War II.

Fig. 5 – Extrait du profil en long de la Bruche couvrant le tronçon étudié (délimité par les traits rouges) et relevé durant la Seconde Guerre Mondiale.

4. Results

4.1. Lateral mobility

The historical lateral mobility of the whole studied reach through the diachronic superposition of the active channels from 1866 to 2015 is represented in two different ways to help visualising the whole breadth of spatio-temporal changes. Whereas the first map displays the subdivision into 38 sub-reaches and overlays all diachronic active channels (fig. 6), the second displays two successive active channels according to the time period elapsed between each planimetric record (fig. 7). Even though representing the geometric error would be irrelevant at this spatial scale, several observations related to lateral activity can be drawn from these qualitative maps. It first suggests sustained lateral migration of the entire reach during the period 1866-1950, as channels during this period hardly overlap each other. It is especially striking along the sub-reach 35, where the amplitude of the largest meander of the whole studied area increased of more than 300 m (from north to south) in less than a hundred years, from 1866 to 1950 (fig. 6). This sustained lateral activity is also observed along sub-reaches 6-7-8 where the river formed a meander between 1866 and 1884, likely followed by a meander cut-off (fig. 7). A second noticeable planform change is observable during the period 1964-1978, particularly along sub-reaches 5 to 14 where active channel switched from a meandering to a more linear channel pattern through two major meander cut-offs (fig. 7). Smaller meander cut-off is also visible during the period 1956-1964 along sub-reaches 19-20. About 500 m downstream (sub-reaches 24-25), the active channel is highly active as well and displayed a cut-off on period 1978-1986. It seems that a second one is about to occur in the near future on sub-reach 25.

By focusing on morphological metrics averaged on the whole studied reach (fig. 8), we observe a strong increase of sinuosity from 1866 (1.65) to 1964 (2.16). Since then, sinuosity has decreased a little and seems fluctuating around 2. As for the mean active channel width, its temporal evolution is less clear, but an overall decreasing trend can be observed from 1866 to 1950 (24.2 to 19.1 m). Since then, the value has fluctuated around 20 m. The approximate inverse correlation of these both variables is noticeable.

Spatial (per sub-reach) and temporal (per time period) evolution

of the AMI (fig. 9) allows pinpointing where and when lateral adjustments precisely took place. The highest and lowest mean AMI along the entire reach are recorded during the periods 1866-1884 (3.4 m.yr^{-1}) and 1986-2011 (0.4 m.yr^{-1}), respectively (fig. 9A). Whilst a mean AMI value of 1.2 m/yr is recorded over the entire period (1866-2015), sub-reaches 35 and 16 are characterised by the highest and lowest mean AMI, with values of 3.8 and 0.3 m.yr^{-1}, respectively (fig. 9B).

Over approximately one century (from 1866 to 1964), lateral morphodynamics seem to have been relatively homogeneously

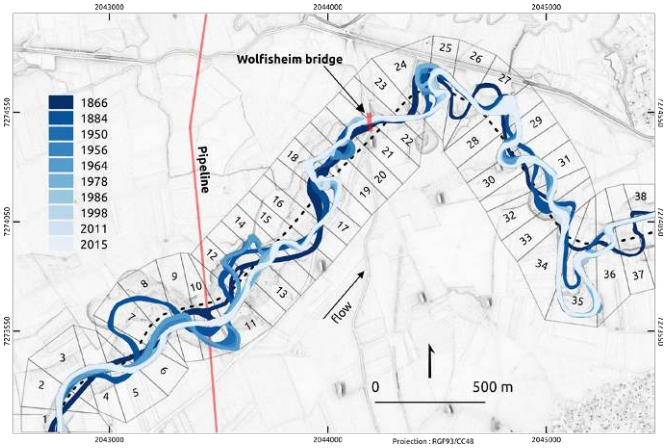

Fig. 6 – Diachronic map of overlaid active channels.

The 38 sub-reaches from which AMI is calculated are represented and numbered. Background corresponds to a Sky View factor visualization of the 2015 LiDAR-derived DTM. Black dashed line refers to the centerline of the historical mobility space.

Fig. 6 – Carte de superposition diachronique de la bande active.

Les 38 tronçons depuis lesquels l'AMI est calculé sont représentés et numérotés. L'arrière-plan correspond à une visualisation Sky View Factor du MNT dérivé du LiDAR 2015. La ligne pointillée noire correspond à la ligne centrale de l'espace de mobilité historique.

distributed along the entire studied reach, although results show some local activity peaks limited in time, such as in sub-reaches 7-8, 20 and 35 during the periods 1866-1884, 1950-1964 and 1866-1956, respectively. Interestingly, between 1964 and 1978, one single major increase is recorded along the sub-reaches 10 to 13 (peak AMI values reaching 10 m.yr^{-1}). From 1978 to 2015, the spatial evolution of lateral mobility is contrasting between sub-reaches 1-17 and 18-38. Whereas the upstream section is characterised by a generalized stability with very low associated AMI values, some activity peaks, anew limited in time, stand out in the downstream section, such as in sub-reaches 18, 25 and 35 where AMI values reached 8.1 (2011-2015), 4.2 (1978-1986) and 5.0 (2011-2015) m.yr^{-1}, respectively.

4.2. Vertical evolution

The vertical evolution of the channel bottom is assessed for two distinct time periods: the secular (by comparing the profile documented at 1940 with that of 2006) and decadal (comparison between 2006 and 2015) timeframe. Note that the studied reach in figure 10 has been extended downstream to the Eckbolsheim bridge (*i.e.,* along ~150 m) to allow the different longitudinal profiles to be fitted horizontally, according to two temporally stable structures (Wolfisheim and Eckbolsheim bridges). As for the general shape of the three channel bottom longitudinal

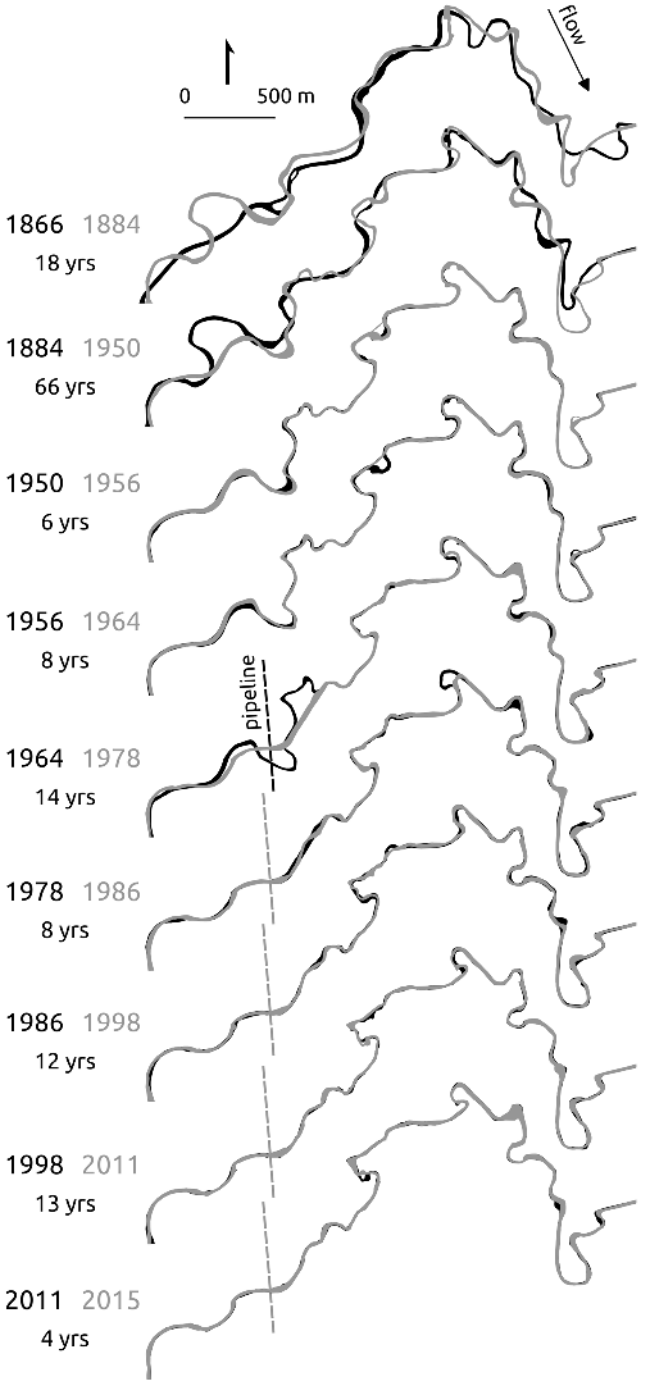

Fig. 7 – Paired diachronic active channels with time period elapsed between each planimetric record.

Fig. 7 – Chenaux actifs chronologiquement couplés avec les pas de temps écoulés entre chaque documentation planimétrique.

profiles (fig. 10), we notice at first glance that the 1940 profile is more irregular, including some counter-slopes, than the smoother LiDAR-extracted channel bottom profiles. This is explained by the fact that the latter are derived from the water surface. At the secular scale, a general and almost ubiquitous riverbed aggradation is indisputably observed: it amounts to ~0.6 m on average. By contrast, slight riverbed degradation has occurred only in the direct vicinity of both bridges. At the decadal scale, whilst the vertical uncertainty related to both

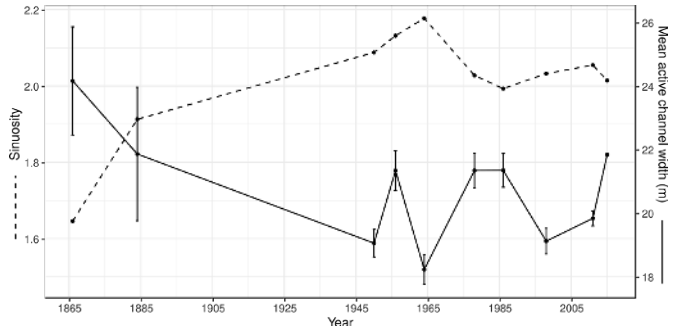

Fig. 8 – Evolution of mean active channel width and sinuosity during the last ~150 years.

Error bars correspond to the respective geometric error values (tab. 1).

Fig. 8 – Évolution de la largeur moyenne de la bande active et de la sinuosité au cours des ~150 dernières années.

Les barres d'erreurs correspondent aux erreurs géométriques respectives (tab. 1).

LiDAR-extracted channel bottom profiles overlap most of the time (*i.e.*, grey buffer zones in fig. 10), a significant aggradation is locally recorded in three zones, with values ranging between 0.1 m (in the very downstream section of our studied reach) and 0.3 m (in the very upstream section and around the pipeline).

Concerning the bank elevation, its evolution is difficult to interpret for two main reasons. First, the bank represented on the 1940 longitudinal profile is unspecified. Second, the planimetric position of the channel has largely evolved from 1940 to nowadays (fig. 6-7, 9), thereby implying a bias in bank elevation variations. Nevertheless, in the vicinity of the Wolfisheim bridge, the 2015 right bank elevation fits particularly well with the 1940 unspecified bank elevation (fig. 10). On a methodological point of view and because the historical lateral dynamic of sub-reaches 21-22 has been relatively low (fig. 6), the strong similarity of the 1940 and 2015 profiles in this area legitimately supports the use of the value of 0.486 m provided by the IGN to convert the elevations in the same datum (EVRF 2000).

5. Discussion

5.1. Methodological uncertainties and implications

The historical approach is prone to result in geomorphological misinterpretations if spatiotemporal uncertainty sources affecting both planimetric and vertical data are not properly considered (Lea and Legleiter, 2016; Donovan et al., 2019). This is especially true when it is applied to mid-sized rivers (Jautzy et al., 2020).

Concerning planimetric uncertainties, geometric error

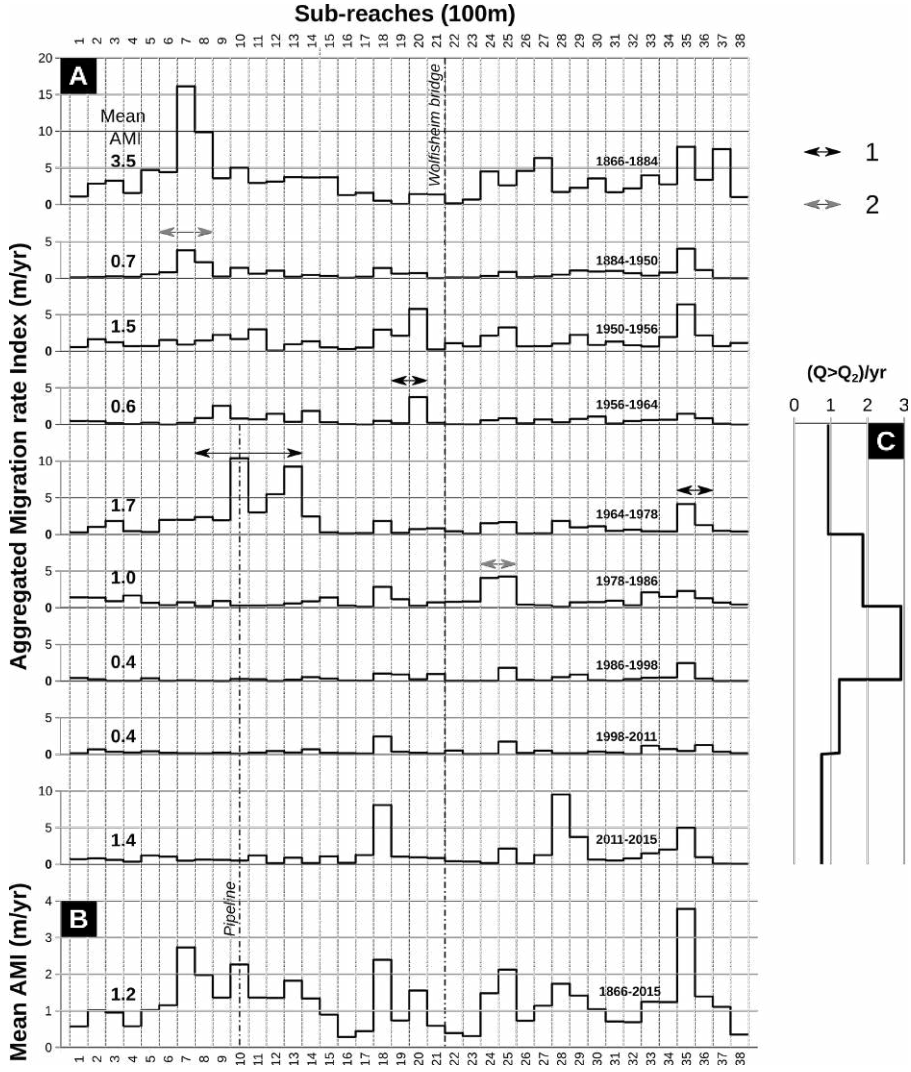

Fig. 9 – Aggregated Migration rate Index (AMI) over the studied reach of the Lower Bruche.

A: AMI per sub-reach and time period. 1. Anthropogenic modification (artificial cut-offs, embankment); 2. Natural meander cut-off. B: Mean AMI per sub-reach between 1866 and 2015. C: number of discharge events exceeding Q2 per year, for each period.

Fig. 9 – Indice agrégé de migration (AMI) sur le tronçon étudié de la Basse Bruche.

A : AMI par tronçon et période. 1. Intervention humaine (recoupements artificiels, remblai); 2. Recoupement naturel. B : AMI moyen par tronçons entre 1866 et 2015. C : Nombre de fois que Q2 a été dépassé par an, pour chaque période.

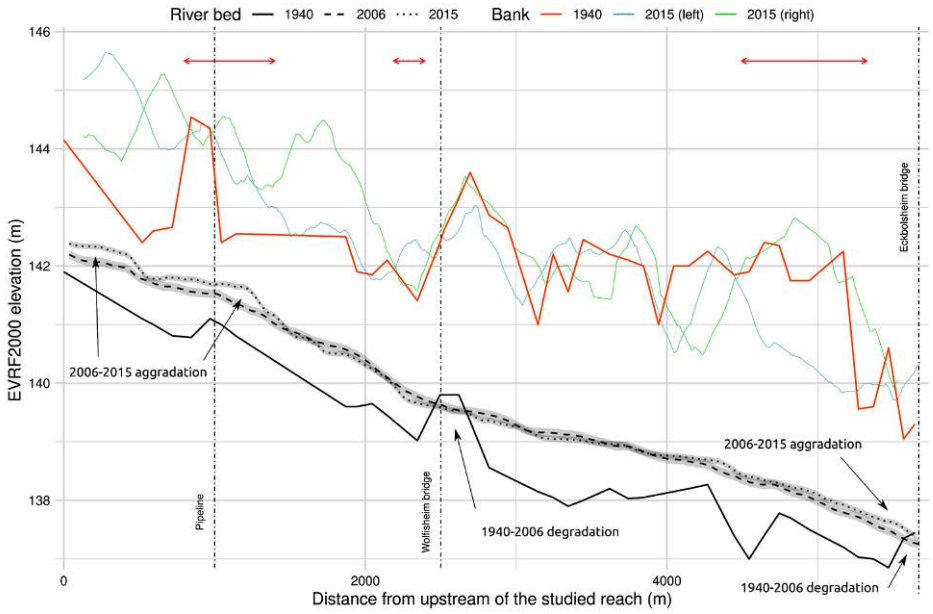

Fig. 10 – Evolution of the longitudinal profile from 1940 to 2015: channel bottom and bank(s).

Buffer of vertical uncertainty on the 2006 and 2015 profiles refers to the vertical precision claimed by the DTMs producers. Red horizontal arrows refer to the location of anthropogenic modifications of the channel, also represented on Figure 9.

Fig. 10 – Évolution du profil en long de 1940 à 2015 : fond du lit et berge(s).

L'incertitude verticale des profils de 2006 et 2015 correspond à la précision verticale annoncée par les producteurs des MNT. Les flèches horizontales rouges correspondent à la position des modifications anthropiques du chenal, également représentées sur la Figure 9.

associated to orthophotos (tab. 1) used in this study are about three times lower than those associated to the co-registered aerial photos implemented by Payraudeau et al. (2010) in the same study area. The availability of high resolution DTMs also allowed reducing the error related to active channel digitization and enhancing the quality of map coregistration, despite the presence of relatively dense riparian vegetation. Moreover, focusing on four sub-reaches in the Lower Bruche, Jautzy et al. (2020) assessed the significance of twelve surficial planform changes, ranging from 0.01 to 0.9 m yr^{-1}, that had occurred between 1950 and 1964. They found that the only non-significant planform change was an eroded/deposited surface with a value of 0.02 $m.yr^{-1}$ ±53.4 %. Although the metric used in this study (AMI) is rougher than that of Jautzy et al. (2020) as it merges eroded and deposited surfaces, the planform changes documented here far exceed the previous values, ranging from 0.4 to 3.4 $m.yr^{-1}$, with a mean AMI value of 1.2 $m.yr^{-1}$ over the 1866-2015 period (fig. 9).

We consequently assume that the planimetric results are robust and sound for geomorphological interpretations, although an uncertainty related to maps must be borne in mind. Indeed, bank contours were digitized just as they are represented on maps and might therefore not represent the actual active channel. Whilst we assume that this uncertainty source does not significantly impact the AMI results because lateral mobility inferred from maps is generally higher (fig. 9A) than the one inferred from orthophotos, it must be considered when one wants interpreting channel width evolution.

Concerning vertical uncertainties, the major potential bias arises from the comparison of channel-bottom profiles obtained by two different methods. Whereas the channel bottom from the 20th century was directly surveyed in the field and thus documents the former thalweg, the LiDAR-derived profiles from the 21st are extrapolated from the water-surface elevation. Even if this second technique cannot assess the bathymetry with the highest accuracy and probably smooths the channel bottom to a certain extent, we argue that secular vertical variations were still captured with enough precision to produce a reliable trend.

5.2. A refined spatiotemporal planform evolution of the Lower Bruche

The planimetric study of Payraudeau et al. (2010) in the Lower Bruche used one map, six aerial photographs and one LiDAR-derived DTM, covering 118 years (1884-2002). By contrast, this study is based on two maps, eight orthophotos and two LiDAR-derived DTMs, covering 149 years (1866-2015). It thus not only takes advantage of a greater pool of resources but also spans a longer time period. Moreover, all photographs used by Payraudeau et al. (2010) have been processed to orthophotos in the meanwhile, leading to a significant decrease of the geometric error (tab. 1). Thanks to the specifically designed AMI which aggregates any type of lateral change into the same metrics, we could thus investigate channel mobility along the whole reach (divided in 38 sub-reaches), instead of exclusively focusing on meander dynamics (twelve sub-reaches) as did Payraudeau et al. (2010). Combined with the enhanced temporal resolution (nine time slices *versus* six), our methodology allowed understanding planform spatiotemporal variations at a much finer scale. Unfortunately, due to our enhanced methodology (AMI) to measure lateral mobility, the migration rates yielded in this study are not readily comparable to those assessed by Payraudeau et al. (2010). Finally, the availability of a second LiDAR-derived DTM and the use of the 1940 longitudinal profile provided a considerable advantage in the understanding of the vertical evolution of the Lower Bruche, a missing key point in the previous study.

5.3. Geomorphological adjustments not primarily controlled by hydrology

Among all drivers of river evolution at the decadal or secular scale, changes in hydrological regimes (mostly governed by climate), especially flood regimes (*e.g.*, Baker et al., 1988), have been long recognized as a key driver of morphodynamic adjustments (Buffington, 2003).

We tested the role of hydrology over the last 50 years through the widely-used, non-parametrical Mann-Kendall test (Mann, 1945; Zar, 2005), using the R package trend (Pohlert, 2020). It allows the

detection of any potential trend in temporal series with indication of its significance. The test was applied to a set of 52 discharge series gauged at Holtzheim located 1.2 km upstream of our studied reach over the 1965-2018 period. Among the series including monthly and annual median, mean, and minimum daily discharges, the only hydrological series with a significant increasing trend (p-value = 0.01) is the annual minimum daily discharge (tab. 2). As the latter focuses on the single minimum daily event occurring every year, it seems very unlikely that the increasing trend observed in this indicator might have had significant impacts on geomorphological adjustments.

As for the recurrence of hydrological events on morphological channel evolution, the 1986-1998 period seems to be the most affected because it records *(i)* the highest annual rate (~3) of Q > Q2 (fig. 9C), and *(ii)* four mean daily discharge values > Q10, one of them even exceeding Q50 (fig. 11). Interestingly, no major lateral adjustment is observed in parallel during this period; it is actually characterized by the lowest mean AMI value (0.4 m.yr^{-1}) over the entire time period considered in this study (1866-2015). Based on both aforementioned arguments, a primary hydrological control on river dynamics of the Lower Bruche over the last 50 years can be reasonably ruled out.

Table 2 - p-value of the Mann-Kendall test performed on 48 monthly and 4 annual discharge series, gauged at Holtzheim.

Tableau 2 – Valeur p du test de Mann-Kendall appliqué sur 48 séries de débits mensuels et 4 annuels, jaugées à Holtzheim.

	Median	Mean	Max	Min
January	0.38	0.58	0.71	0.79
February	0.71	0.96	0.42	0.35
March	0.6	0.68	0.71	0.38
April	0.29	0.27	0.28	0.26
May	0.25	0.29	0.53	0.32
June	0.27	0.52	0.97	0.55
July	0.61	0.97	0.83	0.51
August	0.71	0.95	0.88	0.13
September	0.75	0.8	0.6	0.34
October	0.56	0.67	0.32	0.29
November	0.85	0.71	0.51	0.74
December	0.64	0.52	0.92	0.12
Annual	0.14	0.44	1	**0.01**

The bold value indicates a positive significant trend.

La valeur en gras correspond à une tendance significative positive.

The beginning of the studied period which spans the end of the 19th century is not covered by hydrological series. Interestingly, it matches the end of the Little Ice Age (LIA), which is characterized by transitional hydrological conditions between a flood-dominated and a drought-dominated regime (Carozza et al., 2012). Owing to these changes, the end of the LIA is sometimes assumed to induce a decrease in river dynamics (David et al., 2015, 2016; Jantzi, 2017). The latter is documented in the lower Bruche with a clear decrease in lateral mobility between the end of the 19th (AMI = 3.5 m.yr^{-1}) and the beginning of the 20th century (AMI ~1 m.yr^{-1}). The hydrological transition linked with the end of the LIA is relatively well documented for the Rhine and some of its Vosgian tributaries (Himmelsbach et al., 2015). However, in the absence of paleoflood data or chronostratigraphical evidence for the Bruche river itself, the question whether the end of the LIA controlled the reduced lateral dynamics of the Lower Bruche more than one century ago remains open.

5.4. A diversity of human actions impacting river dynamics

All major changes reported in this study, including channel narrowing (though questionable due to uncertainties, see. §5.1.), the overall increase in sinuosity (fig. 8) and the main lateral and vertical adjustments (fig. 9-10) are more likely driven by human activities.

5.4.1. Lateral adjustments

As for lateral adjustment at the sub-reach scale, we observed a significant change in the lateral activity upstream and downstream the sub-reach 14 (fig. 9), likely due to the underground pipeline. In relation to its erection in 1965 and modification in 1971, an almost complete channel artificialization (both bed and banks) from sub-reach 8 to 13 (fig. 9A) was performed (Maire, 1985). The modifications mostly consisted in *(i)* two man-made cut-offs, one upstream the pipeline crossing and another directly above it, *(ii)* the erection of a ~1.40 m-high weir in which the pipeline was integrated and *(iii)* the linearization of the active channel along ~450 m and its widening (~40 m) downstream the pipeline (sub-reach 11 to 14). Fifteen years after the pipeline construction, the same author observed significant geomorphological adjustments around the pipeline pathway. They include a decrease of local stream velocity from sub-reach 11 to 14 leading to riverbed

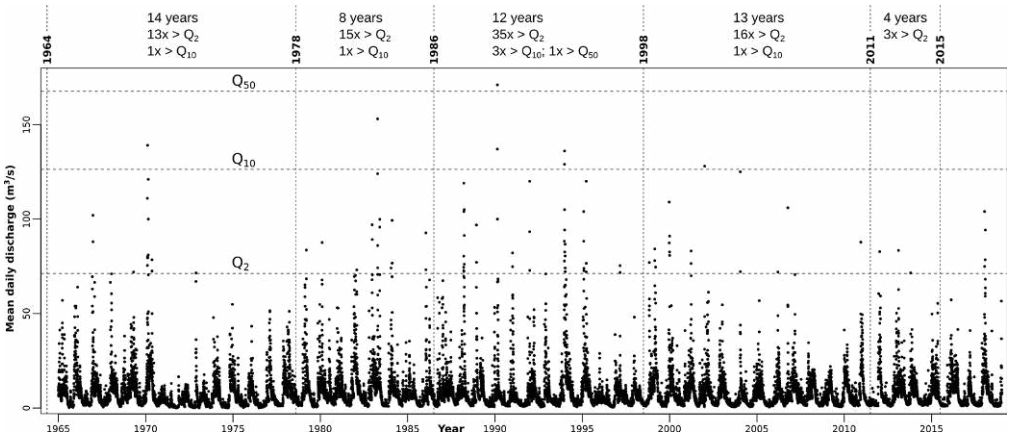

Fig. 11 – Mean daily discharge of the Lower Bruche from 1965 to 2018 at Holtzheim.

Dashed vertical lines represent the years with orthophoto survey.

Fig. 11 – Débits journaliers moyens de la Basse Bruche, de 1965 à 2018 à Holtzheim.

Les lignes pointillées verticales correspondent aux levés orthophotos.

aggradation from sub-reach 8 to 21 (Wolfisheim bridge). The increasing lateral activity observed downstream the pipeline since its construction (fig. 9A) might thus correspond to the river geomorphological response to the artifizialisation of sub-reaches 8 to 13.

In the downstream part of the study area, the meander located in sub-reach 35 (fig. 12), described by Maire (1985) as "one of the kind in Alsace (Eastern France)", illustrates well the significant impact that human activities have had on the Lower Bruche too. This large meander loop obtained its current planform in less than a hundred years (1866-1950), extending itself over more than 300 m (fig. 12A) with a AMI of 6 m.yr^{-1}. Since then, the AMI has halved to 3 m.yr^{-1} in average from 1950 to 2015 as a likely result of improvised embankments, visible on the DTM (fig. 12A) and in the field (fig. 12E). Despite the twofold AMI decrease and its apparent stability, sustained morphogenic processes have been and are still at work in this meander. The diachronic orthophotos reveal a significant migration between 1950 and 1964, at the downstream end of the loop (fig. 12B). Afterwards, a massive embankment (~200 m long) was achieved between 1964 and 1978 (fig. 1C, 12B) and momentarily impeded local erosion. More recently, the LiDAR-DTMs of Difference (DoD) between 2006 and 2015 not only shows almost continuous erosion along the outer bank but also significant bank retreat at the downstream end of the loop (~10 m) and downstream of the meander (fig. 12C-D). This is confirmed by the high AMI (~5 m.yr^{-1}) recorded in the sub-reach 35 between 2011 and 2015 (fig. 9).

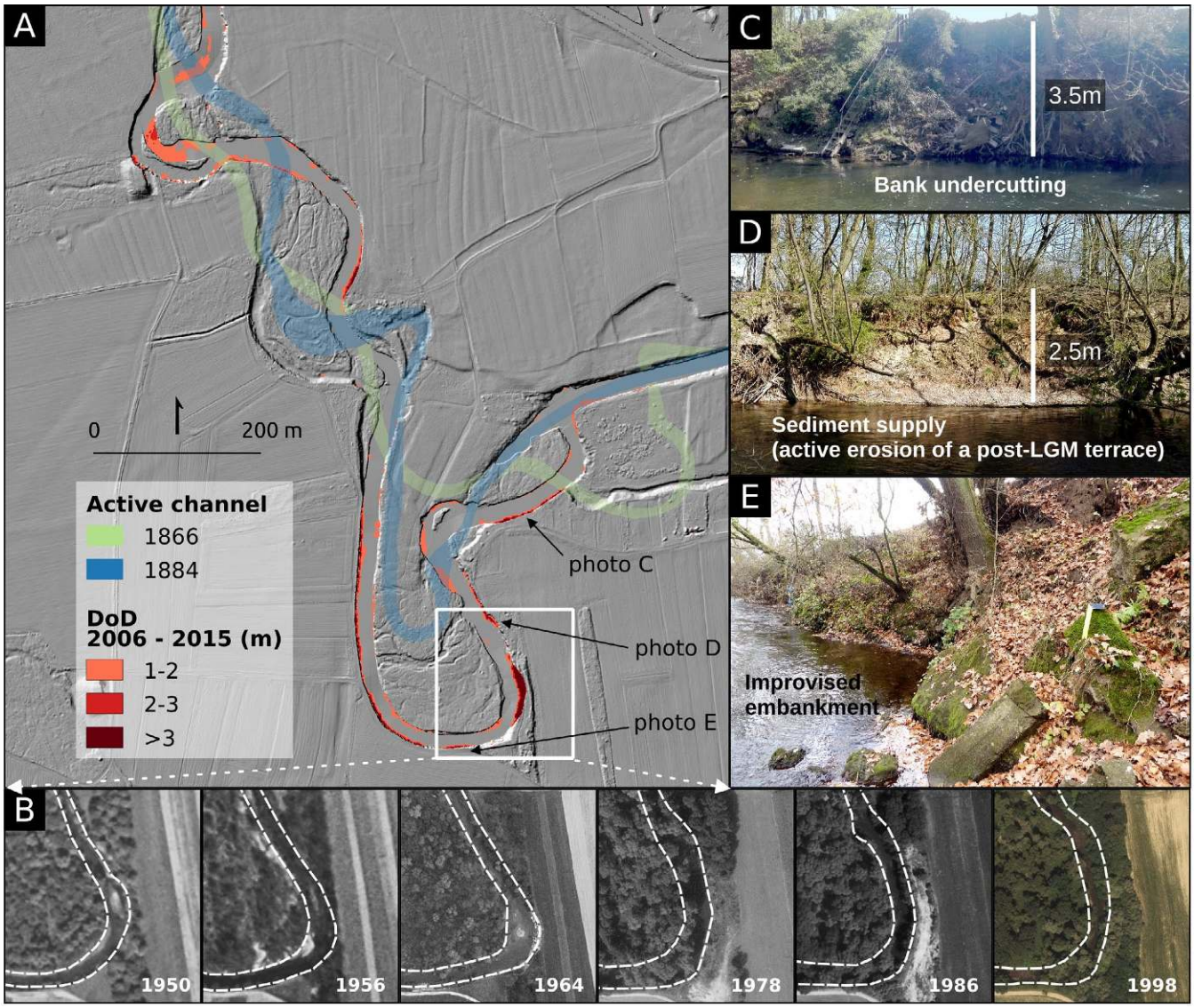

Fig. 12 – Historical evolution of the downstream part of the studied reach along with current processes.

A: planform evolution of the active channel during the end of the 19th century. Recent erosion is computed by a 2006-2015 DTMs of Difference (DoD). Background corresponds to the 2015 hill-shaded LiDAR. B: planform evolution of the downstream curvature of the meander loop during the second half of the 20th century. C, D: field photos showing undercutting processes along a heavily modified bank and a natural bank (lower terrace) with local sediment supply, respectively. E: improvised embankment of pluridecimetric anthropogenic blocks impeding bank erosion.

Fig. 12 – Évolution historique de la partie aval de la zone d'étude et mise en évidence de processus actuels.

A : évolution planimétrique du lit actif pendant la fin du XIXe siècle. L'érosion récente est mise en valeur par un différentiel de MNT 2006-2015. L'arrière-plan correspond au LiDAR 2015 ombragé. B : évolution planimétrique de l'aval de la courbure du méandre lobé pendant la seconde moitié du XXe siècle. C, D : photos de terrain montrant du sapement à la base respectivement dans une berge profondément modifiée et une berge naturelle (basse terrasse) avec approvisionnement sédimentaire local. E : "enrochement" non-planifié de blocs anthropiques pluridécimétriques limitant l'érosion de berge.

5.4.2. Vertical adjustments

The most striking result undoubtedly is the (almost) generalized, ~0.6 m-high aggradation recorded at the secular scale along the whole studied reach (fig. 10). It is somehow unexpected as it seemingly contradicts the common trend observed for European rivers which are largely affected by historical channel incision (Rinaldi, 2003; Simon and Rinaldi, 2006).

According to Lane's balance, one would anticipate river bed aggradation when a decrease of the stream transport capacity or, alternatively, an increase in sediment supply and associated bedload transport, occurs (e.g. Dust and Wohl, 2012). To test the first condition, we computed the evolution of the specific stream power ω through time (fig. 13), based on the following equation (Leopold, 1992; Charlton, 2008):

$$\omega = (\rho g Q S) / W \quad [4]$$

ρ is the density of water (1000 kg/m³) and g the gravitational constant (9.8 m/s²). We considered Q2 as the bankfull discharge (Q) and used the planimetric data to document the evolution of the channel width (W) and the thalweg length. The slope (S) is measured from the 2015 LiDAR and thus assumed to be constant through time (5 m of elevation drop in the studied reach). No temporal pattern is observed (fig. 13). In addition, the sole significant hydrological trend observed over a decadal scale is the increase of the annual minimum daily discharge (see section 5.3.). This is largely insufficient to suggest an hypothetical decrease of transport capacity and leaves this question open.

Investigating the second condition requires looking at the two distinct geographical areas where a possible increase in sediment delivery could have occurred over historical times. They are: *(i)* the Lower Bruche via the reworking of older sedimentary deposits inducing local sediment supply and *(ii)* the Upper Bruche catchment draining the Vosges (*i.e.*, the distant source; see section 2.1.). As for the first area, sustained outer bank retreat, mostly associated to meander development, locally erodes alluvial sediments originating either from the Holocene floodplain (fig. 2A) or the post-LGM terrace (fig. 12D), thereby injecting coarse material into the active channel. This induces the formation of bars downstream, which may enhance bank erosion and, finally, channel widening which can induce sediment deposition (Malavoi and Bravard, 2010; Chardon et al., 2021). It remains however unsure whether this process is able to ensure a generalized channel aggradation along the whole studied reach. Precise sediment budgeting, which is beyond the scope of this study, would help answering this question.

As for the second area, we assume that the most recent deforestation phase in the Vosges Massif, which took place during the 18th century (Gebhardt et al., 2015), probably triggered the last, massive pulse of sediment production on the hillslopes of the Upper Bruche catchment. In this respect, based on radioactive tracers in pebbles with a recovery rate of 65% in the Bruche headwaters, a yearly *(i.e.,* over 15 months) maximal transport distance of 350 m for the bedload linked to three flood events was recorded (Courtois et al., 1970). If we average this value over a secular timescale, bedload would have been transported downstream over several tens of kilometers (up to 50-60 km over two centuries). Interestingly, this value roughly matches the distance between the Upper Bruche and our study area. This inference suffers from two limitations. First, the unavailability of a long-term bedload monitoring on more than three flood events makes this averaged transport rate over longer timescales somewhat speculative. Second, a potential significant time lag in sediment connectivity, involving a temporary storage of sediments on deforested hillslopes, is not considered. The question whether secular riverbed aggradation results from an upstream erosional signal linked to deforestation thus remains open. Similar further research focusing on river dynamics in upstream reaches of the Bruche and other Vosgian tributaries would help unravelling this issue.

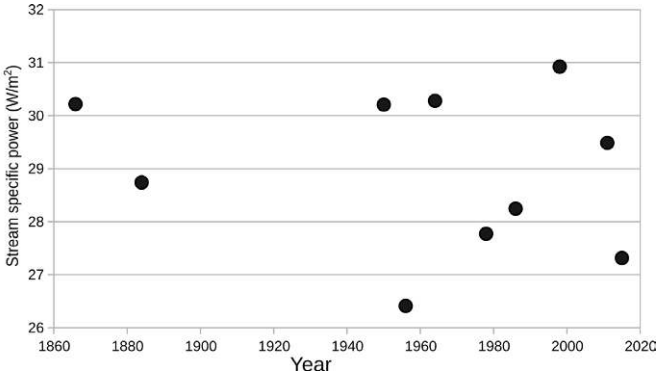

Fig. 13 – Evolution of the stream specific power, calculated in the study reach from planimetric data (thalweg length and channel width).

Fig. 13 – Évolution de la puissance spécifique du cours d'eau, calculée sur le tronçon à l'étude à partir des données planimétriques (longueur du thalweg et largeur du chenal).

The whole hydrological network of the Bruche catchment is currently affected by around four hundred different kinds of weirs (Sandre referential of flow obstacles, OFB). Whilst it is widely acknowledged that dam or weir removal can induce upstream aggradation (Bednarek, 2001), little is known about intentional removal or progressive deterioration over time of the numerous weirs present along the Bruche's network. Whether the progressive release of sediments previously stored upstream of weirs, notably those linked to former mills, is responsible for the downstream aggradation on a secular time frame remains open too. Further investigations, using Radio Frequency IDentification (RFID) tags (Casserly et al., 2020; Galia et al., 2021) and/or iron slags (Peeters et al., 2020) as short and long-term tracers of bedload dynamics in relation to the presence (or removal) of weirs could be helpful to unravel this question.

Finally, the decadal-scale evolution of the riverbed profile highlights three localized aggradation areas of limited amplitude around 10-30 cm (fig. 10). Although a 30 cm aggradation can correspond to a single hydrological event, the two reaches recording the highest aggradation are located up- and downstream the pipeline (fig. 10), thereby possibly pointing to its sustained influence on fluvial morphodynamics more than 50 years after its construction.

5.5. Comparison of the Lower Bruche's lateral dynamics with similar rivers

This study precisely quantifies the lateral and vertical dynamics of an alluvial reach of the Lower Bruche over the last 200 years. As specified in section 2.3., the studied reach is categorized as a "river

with moderate energy and high lateral dynamics" (Schmitt et al., 2007). By contrast, if we exclusively focus on its specific stream power (~27 W/m²), the studied reach could be classified as a low energy river, as it falls in the theoretical lower range usually reported in the literature between laterally active and inactive reaches 25–35 W/m² (Brookes, 1987; Orr et al., 2008; Bizzi and Lerner, 2015; Dépret et al., 2017). This slight inconsistency raises the question: In terms of lateral dynamics, where does the Lower Bruche stand in comparison with similar rivers?

We thus briefly compare the values of migration rates along the studied reach with those reported from similar reaches in French rivers. Although such observations globally remain sparse on rivers of low to moderate energy, a few studies recently focused on low-energy alluvial reaches in western France: the Cher (Dépret, 2015; 2017), the Seulles (Lespez, 2015; Beauchamp, 2017), the Merantaise (Jugie, 2018), the Charente (Duquesne, 2020) and the Loire (Corbonnois, 2016). All these studies reported a specific stream power ranging from 10 to 40 W/m², an active channel width ranging from 10 to 40 m and mean migration rate values lower than 0.5 m/yr. This contrasts with the mean value more than twice higher in our studied reach 1.2 m.yr (fig. 9A), with a specific stream power of 27 W/m² and an active channel width of ~20 m.

Even though a bias might arise from the comparison of migration rates computed via different methodologies and over different time periods, we consider that this difference is significant and highlights the relatively high lateral mobility of the Lower Bruche. However, one must keep in mind that this dissimilarity between the Lower Bruche and the other rivers does not integrate prime-order factors controlling lateral mobility. First, the bank composition of some of the fluvial reaches in Western France seems to be more cohesive than those of the Lower Bruche (section 2.3.). Fining upward sequences mostly characterize bank composition in our studied reach. Loose sandy and gravelly sediments left by former channel activity, either in the Holocene floodplain or the post-LGM terrace, are overlain by more cohesive silty loam typical of overbank deposition (fig. 14A). Therefore, concave banks are prone to the cycle of bank retreat processes depicted by Brierley and Fryirs (2013), which could be witnessed during our field investigations. It successively involves basal erosion, mass failure, toe accumulation and removal of the collapsed sediments during the next flood event(s) (fig. 14B). The cohesiveness of bank material is acknowledged to be one of the main controlling factors on the mobility of low-energy alluvial rivers (Candel et al., 2020). The erodibility of bank material in the Lower Bruche can thus play a prevailing role and explain its high lateral dynamics. Second, it is necessary to keep in mind that the upper Bruche catchment drains the Vosges Massif before debouching into the Rhine alluvial plain. This makes the context of the alluvial section very specific compared to the rivers of Western France mentioned above. The wide valley of the Lower Bruche bears witness of a complex mix of fan deposits and a system of sandy/gravely alluvial terraces (Maire, 1966). Third, variable riparian vegetation, which is largely recognized as a significant controlling factor of bank erosion (Hey and Thorne, 1986; Millar, 2000), may also explain differences of mean channel migration rates. Finally, some authors also pointed out the potential impact of neotectonics, as the Lower Bruche is located in the direct vicinity of a main normal fault system of the Upper Rhine Graben (Maire, 1967; Vogt, 1992). However, no clear evidence of tectonic activity could be highlighted and linked to the Late Quaternary evolution of this river system.

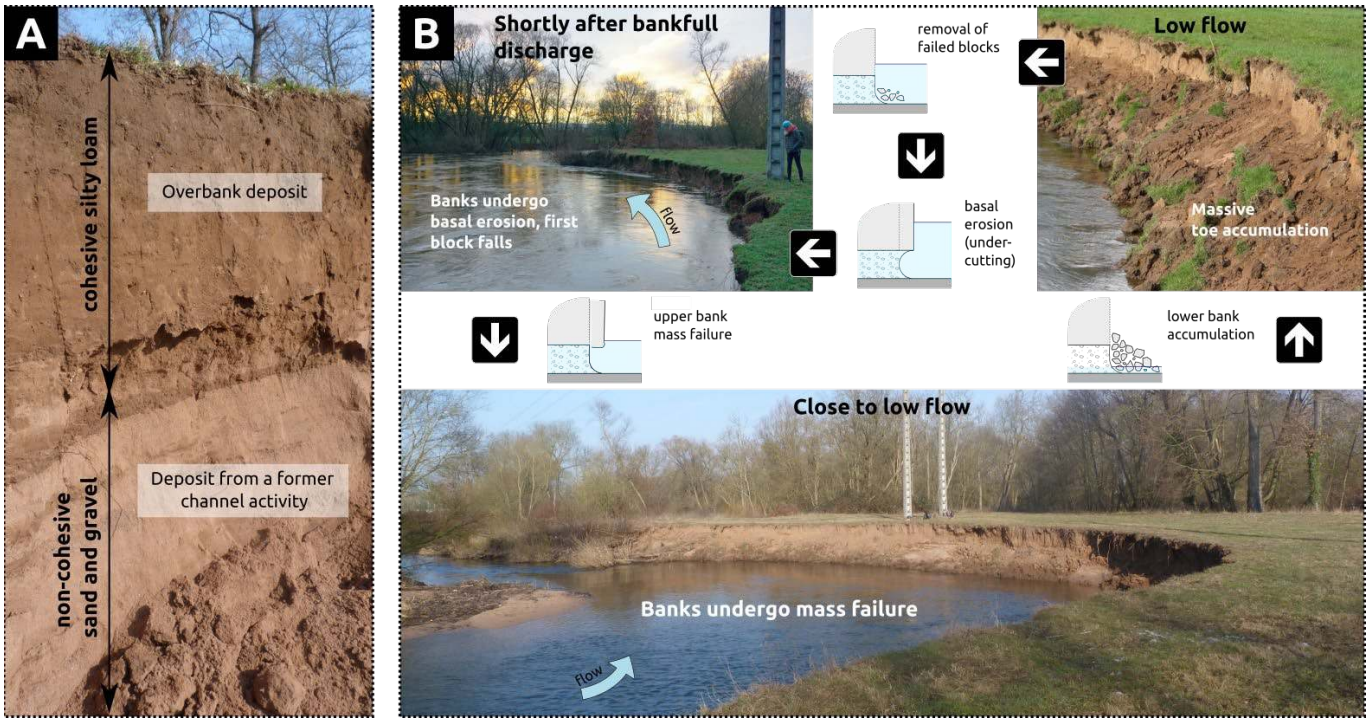

Fig. 14 – The cyclical process of bank retreat (Brierley and Fryirs, 2013) involved in the studied reach of the Lower Bruche.
A: Profile of the composite concave bank. B: Photographic and schematic illustration of the cyclical process of bank retreat in the sub-reach 25.

Fig. 14 – Le cycle de retrait de berges (Brierley et Fryirs, 2013) impliqué dans le tronçon à l'étude de la Basse-Bruche.
A : Profil de la berge concave composite. B : Illustration photographique et schématique du cycle de retrait de berges dans le tronçon 25.

6. Conclusion

This study demonstrates the usefulness of jointly analyzing a large set of both planimetric (maps and orthophotos) and vertical (longitudinal profile and LiDAR) diachronic data to accurately reconstruct the evolutionary trajectory of a dynamic 6 km-long reach of the Lower Bruche with a high resolution over 150 years. Although using ancient data sources (*i.e.,* maps and field surveys) requires a thorough consideration of related uncertainties, we successfully show that their combination with accurate recent data (orthophoto, LiDAR) is relevant to quantify lateral and vertical channel morphodynamics on decadal and secular timescales. In this respect, the specifically-designed indicator of lateral mobility, which aggregates the various types and origins of planform changes into a single index (AMI), has proven its effectiveness and can be easily transferred to other wandering rivers. The evolutionary trajectory of the Lower Bruche reveals a high and almost generalized lateral mobility from the mid-19th to the mid-20th century with mean AMI ranging from 0.6 to 3.5 m.yr^{-1}. Then, a major man-induced modification of a sub-reach, *i.e.,* the construction of an underground pipeline, dramatically reduced the intensity of the lateral morphodynamics upstream (and possibly increased it a little downstream), leading to a mean AMI ranging between 0.4 and 1.4 m.yr^{-1}. In other sub-reaches, the lateral mobility of the river has been primarily controlled by various anthropogenic actions (*e.g.*, embankments, channelisation). As for the vertical evolution of the Lower Bruche, the channel elevation shows an average aggradation of ~0.6 m from the mid-20th to the beginning of the 21st century. Although some preliminary explanations could be proposed, such as local sediment reworking and past deforestation in the downstream and upstream parts of the catchment, respectively, or sediment release following weir removal, those remain speculative and require further investigations to be validated. In the Lower Bruche, one could take advantage of established tracing methods, such as slags (Peeters et al., 2020) since this catchment was one "hotspot" of metallurgical activity from the Middle Ages to the Early Modern Period in the Vosges Massif (Mariet et al., 2018). Finally, this spatiotemporal analysis of the historical geomorphological adjustments of the Lower Bruche could greatly help future management projects, all the more meaningful given the high significance of this river in ecological terms. The detailed portrait depicted in this dynamic river reach could represent a strong basis for restoration projects in other strongly impacted reaches of the Bruche or similar Vosgian rivers.

Acknowledgements

This research has been supported by the Scientific Council of the National School for Water and Environmental Engineering of Strasbourg (ENGEES, France). We thank both anonymous reviewers for their constructive remarks. We thank Grégoire Skupinski (LIVE) for providing planimetric data. We also thank Eckhard Wirbelauer for helping with the identification and dating of the german longitudinal profile. This work has been entirely produced with free and open-source programs (QGIS, R, GDAL, Inkscape, Zotero and LibreOffice).

References

Armaș I., Gogoașe Nistoran D.E., Osaci-Costache G., Brașoveanu L. (2013) - Morpho-dynamic evolution patterns of Subcarpathian Prahova River (Romania). CATENA, 100, 83–99. DOI : 10.1016/j.catena.2012.07.007

Arnaud F., Piégay H., Schmitt L., Rollet A.J., Ferrier V., Béal D. (2015) - Historical geomorphic analysis (1932–2011) of a by-passed river reach in process-based restoration perspectives: The Old Rhine downstream of the Kembs diversion dam (France, Germany). Geomorphology, 236, 163–177. DOI : 10.1016/j.geomorph.2015.02.009

Arnaud F., Schmitt L., Johnstone K., Rollet A.-J., Piégay H. (2019) - Engineering impacts on the Upper Rhine channel and floodplain over two centuries. Geomorphology, 330, 13–27. DOI : 10.1016/j.geomorph.2019.01.004

Baena-Escudero R., Rinaldi M., García-Martínez B., Guerrero-Amador I.C., Nardi L. (2019) - Channel adjustments in the lower Guadalquivir River (southern Spain) over the last 250 years. Geomorphology, 337, 15–30. DOI : 10.1016/j.geomorph.2019.03.027

Baillie M.B., Salant N.L., Schmidt J.C. (2011) - Using a historical aerial photograph analysis to inform trout habitat restoration efforts. Earth Surface Processes and Landforms, 36 (12), 1693–1702. DOI : 10.1002/esp.2196

Baker V., Kochel R.C., Patton P.C. (Eds.) (1988) - Flood geomorphology. Wiley-Interscience, New-York, 503 p.

Baulig H. (1922) - Questions de morphologie vosgienne et rhénane. (Premier article). Annales de géographie, 31 (170), 132–154. DOI : 10.3406/geo.1922.10257

Beauchamp A., Lespez L., Rollet A.-J., Germain-Vallée C., Delahaye D. (2017) - Les transformations anthropiques d'un cours d'eau de faible énergie et leurs conséquences, approche géomorphologique et géoarchéologique dans la moyenne vallée de la Seulles, Normandie. **Géomorphologie : relief, processus, environnement**, 23 (2), 121–138. DOI : 10.4000/geomorphologie.11702

Bednarek A.T. (2001) - Undamming Rivers: A Review of the Ecological Impacts of Dam Removal. Environmental Management, 27 (6), 803–814. DOI : 10.1007/s002670010189

Biron P.M., Buffin-Bélanger T., Larocque M., Choné G., Cloutier C.-A., Ouellet M.-A., Demers S., Olsen T., Desjarlais C., Eyquem J. (2014) - Freedom Space for Rivers: A Sustainable Management Approach to Enhance River Resilience. Environmental Management, 54 (5), 1056–1073. DOI : 10.1007/s00267-014-0366-z

Biron P.M., Choné G., Buffin-Bélanger T., Demers S., Olsen T. (2013) - Improvement of streams hydro-geomorphological assessment using LiDAR DEMs. Earth Surface Processes and Landforms, 38 (15), 1808–1821. DOI : 10.1002/esp.3425

Bizzi S., Lerner D.N. (2015) - The Use of Stream Power as an Indicator of Channel Sensitivity to Erosion and Deposition Processes. River Research and Applications, 31 (1), 16–27. DOI : 10.1002/rra.2717

Bravard J.-P. (1989) - La métamorphose des rivières des Alpes fran-

çaises à la fin du Moyen Âge et à l'époque moderne. Bulletin de la Société géographique de Liège, 25, 145–157.

Bravard J.-P. (2017) - Evolution of River Channels and Floods: A Short- to Long-Term Perspective. In Vinet, F. (Eds.): Floods. Elsevier, 149–165.
DOI : 10.1016/B978-1-78548-268-7.50009-2

Brierley G.J., Fryirs K.A. (2013) - Geomorphology and river management: applications of the river styles framework. John Wiley & Sons, 412 p.

Brookes A. (1987) - River channel adjustments downstream from channelization works in England and Wales. Earth Surface Processes and Landforms, 12 (4), 337–351.
DOI : 10.1002/esp.3290120402

Brown A.G., Lespez L., Sear D.A., Macaire J.-J., Houben P., Klimek K., Brazier R.E., Van Oost K., Pears B. (2018) - Natural vs anthropogenic streams in Europe: History, ecology and implications for restoration, river-rewilding and riverine ecosystem services. Earth-Science Reviews, 180, 185–205.
DOI : 10.1016/j.earscirev.2018.02.001

Buffington J. (2003) - Changes in channel morphology over human time scales. In Church, M., Biron, P.M., Roy, A.G. (Eds.): Gravel-Bed Rivers: Processes, Tools, Environments. John Wiley & Sons, Chichester, UK, 435–463.
DOI : 10.1002/9781119952497.ch32

Buraczynski J., Butrym J. (1984) - La datation des loess du profil d'Achenheim (Alsace) à l'aide de la méthode de thermoluminescence. Quaternaire, 21 (4), 201–209.
DOI : 10.3406/quate.1984.1514

Candel J.H.J., Makaske B., Kijm N., Kleinhans M.G., Storms J.E.A., Wallinga J. (2020) - Self-constraining of low-energy rivers explains low channel mobility and tortuous planforms. The Depositional Record, 6 (3), 648–669.
DOI : 10.1002/dep2.112

Carozza J.-M., Puig C., Odiot T., Valette P., Passarrius O. (2012) - Lower Mediterranean plain accelerated evolution during the Little Ice Age: Geoarchaeological insight in the Tech basin (Roussillon, Gulf of Lion, Western Mediterranean). Quaternary International, 266, 94–104.
DOI : 10.1016/j.quaint.2011.06.049

Casserly C.M., Turner J.N., O'Sullivan J.J., Bruen M., Bullock C., Atkinson S., Kelly-Quinn M. (2020) - Impact of low-head dams on bedload transport rates in coarse-bedded streams. Science of The Total Environment, 716, 136908.
DOI : 10.1016/j.scitotenv.2020.136908

Castela P., Tricart J. (1958) - Une coupe typique du cône de déjections nivo-périglacialre de la Bruche: La carrière Zimmer à Lingolsheim. Sciences Géologiques, bulletins et mémoires, 11 (2), 3–14.
DOI : 10.3406/sgeol.1958.1178

Cavalli M., Tarolli P., Marchi L., Dalla Fontana G. (2008) - The effectiveness of airborne LiDAR data in the recognition of channel-bed morphology. CATENA, 73 (3), 249–260.
DOI : 10.1016/j.catena.2007.11.001

Chardon V., Schmitt L., Arnaud F., Piégay H., Clutier A. (2021) - Efficiency and sustainability of gravel augmentation to restore large regulated rivers: Insights from three experiments on the Rhine River (France/Germany). Geomorphology, 380, 107639.
DOI : 10.1016/j.geomorph.2021.107639

Charlton R. (2008) - Fundamentals of fluvial geomorphology. Routledge, Abingdon, UK, 234 p.

Chen B., Krajewski W.F., Goska R., Young N. (2017) - Using LiDAR surveys to document floods: A case study of the 2008 Iowa flood. Journal of hydrology, 553, 338–349.
DOI : 10.1016/j.jhydrol.2017.08.009

Comiti F., Da Canal M., Surian N., Mao L., Picco L., Lenzi M.A. (2011) - Channel adjustments and vegetation cover dynamics in a large gravel bed river over the last 200 years. Geomorphology, 125 (1), 147–159.
DOI : 10.1016/j.geomorph.2010.09.011

Corbonnois J., Bonnefond M., Chardon V., Rodrigues S., Jugé P., Cali J., Verdun J., Simonetto E., Tchekpo W., Labergerie E., Faucheux G. (2016) - Détermination des conditions de la dynamique fluviale d'une rivière aménagée de basse énergie, à partir de secteurs du Loir (Bassin de la Loire aval). Géomorphologie : relief, processus, environnement, 22 (4), 345–361.
DOI : 10.4000/geomorphologie.11559

Courtois G., Gasnier M., Maire M., Scherrer M. (1970) - Étude de déplacements de galets radioactifs sur la Bruche. Comparaison des résultats expérimentaux obtenus et de l'application de la formule de Meyer-Peter. La Houille Blanche, (7), 651–657.
DOI : 10.1051/lhb/1970046

David M., Carozza J.-M., Valette P., Llubes M., Py V., Groparu T. (2015) - Évolution de la dynamique fluviale de la moyenne Garonne toulousaine : apport d'une approche multi-sources cartes historiques, stratigraphie et géophysique sur le site Grenade-Ondes. Géomorphologie : relief, processus, environnement, 21 (1), 21–44.
DOI : 10.4000/geomorphologie.10834

David M., Labenne A., Carozza J.-M., Valette P. (2016) - Evolutionary trajectory of channel planforms in the middle Garonne River (Toulouse, SW France) over a 130-year period: Contribution of mixed multiple factor analysis (MFAmix). Geomorphology, 258, 21–39.
DOI : 10.1016/j.geomorph.2016.01.012

Dépret T., Gautier E., Hooke J., Grancher D., Virmoux C., Brunstein D. (2015) - Hydrological controls on the morphogenesis of low-energy meanders (Cher River, France). Journal of Hydrology, 531, 877–891.
DOI : 10.1016/j.jhydrol.2015.10.035

Dépret T., Gautier E., Hooke J., Grancher D., Virmoux C., Brunstein D. (2017) - Causes of planform stability of a low-energy meandering gravel-bed river (Cher River, France). Geomorphology, 285, 58–81.
DOI : 10.1016/j.geomorph.2017.01.035

Dey S. (2014) - Fluvial Processes: Meandering and Braiding. In Fluvial Hydrodynamics. Springer Berlin Heidelberg, Berlin, Heidelberg, 529–562.
DOI : 10.1007/978-3-642-19062-9_9

Donovan M., Belmont P., Notebaert B., Coombs T., Larson P., Souffront M. (2019) - Accounting for uncertainty in remotely-sensed measurements of river planform change. Earth-Science Reviews, 193, 220–236.
DOI : 10.1016/j.earscirev.2019.04.009

Donovan M., Miller A., Baker M., Gellis A. (2015) - Sediment con-

tributions from floodplains and legacy sediments to Piedmont streams of Baltimore County, Maryland. Geomorphology, 235, 88–105.
DOI : 10.1016/j.geomorph.2015.01.025

Downward S., Gurnell A., Brookes A. (1994) - A methodology for quantifying river channel planform change using GIS. IAHS Publications-Series of Proceedings and Reports-Intern Assoc Hydrological Sciences, 224, 449–456.

Dufour S., Rinaldi M., Piégay H., Michalon A. (2015) - How do river dynamics and human influences affect the landscape pattern of fluvial corridors? Lessons from the Magra River, Central–Northern Italy. Landscape and Urban Planning, 134, 107–118.
DOI : 10.1016/j.landurbplan.2014.10.007

Duquesne A., Plumejeaud-Perreau C., Carozza J.-M. (2020) - Trajectoire d'évolution d'un cours d'eau à très faible énergie : le cas de la Charente entre Angoulême et Saintes (Ouest de la France). Géomorphologie : relief, processus, environnement, 26 (2).
DOI : 10.4000/geomorphologie.14411

Dust D., Wohl E. (2012) - Conceptual model for complex river responses using an expanded Lane's relation. Geomorphology, 139–140, 109–121.
DOI : 10.1016/j.geomorph.2011.10.008

Ertlen D., Schneider N. (2018) - Séquences sédimentaires du pléistocène supérieur et de l'holocène : données récentes dans la partie alsacienne du fossé rhénan supérieur (France). Quaternaire, 29, 149–167.
DOI : 10.4000/quaternaire.8903

Eschbach D., Schmitt L., Imfeld G., May J.-H., Payraudeau S., Preusser F., Trauerstein M., Skupinski G. (2018) - Long-term temporal trajectories to enhance restoration efficiency and sustainability on large rivers: an interdisciplinary study. Hydrology and Earth System Sciences, 22 (5), 2717–2737.
DOI : 10.5194/hess-22-2717-2018

Galia T., Škarpich V., Ruman S. (2021) - Impact of check dam series on coarse sediment connectivity. Geomorphology, 377, 107595.
DOI : 10.1016/j.geomorph.2021.107595

Gebhardt A., Schwartz D., Ertlen D., Campaner A., Meyer N., Langohr R. (2015) - Impacts des anciennes activités humaines dans les sols vosgiens actuellement sous couvert forestier. Revue du Nord, Collection Archéologie (hors série) (23), 59–72.

Gerlier M., Roche P. (1998) - A radio telemetry study of the migration of Atlantic salmon (Salmo salar L.) and sea trout (Salmo trutta trutta L.) in the upper Rhine. In Lagardère, J.-P., Anras, M.-L.B., Claireaux, G. (Eds.): Advances in Invertebrates and Fish Telemetry. Springer Netherlands, Dordrecht, 283–293.
DOI : 10.1007/978-94-011-5090-3_32

Gregory K.J. (2019) - Human influence on the morphological adjustment of river channels: The evolution of pertinent concepts in river science. River Research and Applications, 35, 1097–1106.
DOI : 10.1002/rra.3455

Guéry F. (1962) - Agriculture et industrie dans les Vosges alsaciennes. Revue Géographique de l'Est, 2 (4), 327–344.
DOI : 10.3406/rgest.1962.1801

Gurnell A.M., Downward S.R., Jones R. (1994) - Channel planform change on the River Dee meanders, 1876–1992. Regulated Rivers: Research & Management, 9 (4), 187–204.
DOI : 10.1002/rrr.3450090402

Haettel G., Haettel J.-P. (2012) - Le canal de la Bruche: de Vauban à nos jours. Éditions Coprur, 71 p.

Hawley R.J., Bledsoe B.P., Stein E.D., Haines B.E. (2012) - Channel Evolution Model of Semiarid Stream Response to Urban-Induced Hydromodification. JAWRA Journal of the American Water Resources Association, 48 (4), 722–744.
DOI : 10.1111/j.1752-1688.2012.00645.x

Hey R.D., Thorne C.R. (1986) - Stable channels with mobile gravel beds. Journal of Hydraulic engineering, 112 (8), 671–689.
DOI : 10.1061/(ASCE)0733-9429(1986)112:8(671)

Himmelsbach I., Glaser R., Schoenbein J., Riemann D., Martin B. (2015) - Reconstruction of flood events based on documentary data and transnational flood risk analysis of the Upper Rhine and its French and German tributaries since AD 1480. Hydrology and Earth System Sciences, 19 (10), 4149–4164.
DOI : 10.5194/hess-19-4149-2015

Hughes M.L., McDowell P.F., Marcus W.A. (2006) - Accuracy assessment of georectified aerial photographs: implications for measuring lateral channel movement in a GIS. Geomorphology, 74 (1–4), 1–16.
DOI : 10.1016/j.geomorph.2005.07.001

Jantzi H., Carozza J.-M., Probst J.-L., Valette P. (2017) - Ajustements géomorphologiques du chenal de la moyenne Garonne en aval de Toulouse au cours des 200 dernières années (sud-ouest, France). Géomorphologie : relief, processus, environnement, 23 (2).
DOI : 10.4000/geomorphologie.11692

Jautzy T., Herrault P.-A., Chardon V., Schmitt L., Rixhon G. (2020) - Measuring river planform changes from remotely sensed data – a Monte Carlo approach to assessing the impact of spatially variable error. Earth Surface Dynamics, 8 (2), 471–484.
DOI : 10.5194/esurf-8-471-2020

Jugie M., Gob F., Virmoux C., Brunstein D., Tamisier V., Le Coeur C., Grancher D. (2018) - Characterizing and quantifying the discontinuous bank erosion of a small low energy river using Structure-from-Motion Photogrammetry and erosion pins. **Journal of Hydrology**, 563, 418–434.
DOI : 10.1016/j.jhydrol.2018.06.019

Klein T. (2005) - Dynamique fluviale d'un cours d'eau fortement anthropisé : la Bruche du 17ème siècle à nos jours. Master's Thesis. Université de Strasbourg, Faculté de géographie et d'aménagement, 84 p.

Lallias-Tacon S., Liébault F., Piégay H. (2014) - Step by step error assessment in braided river sediment budget using airborne LiDAR data. Geomorphology, 214, 307–323.
DOI : 10.1016/j.geomorph.2014.02.014

Largiader C.R., Guyomard R., Roche P. (1996) - Mise en évidence de la reproduction naturelle du saumon atlantique (Salmo salar L.) dans un affluent français du Rhin par analyse génétique d'oeufs prélevés dans des frayères. Bulletin Français de la Pêche et de la Pisciculture, (343), 183–188.
DOI : 10.1051/kmae:1996015

Lautridou J.-P., Sommé J., Heim J., Puisségur J.-J., Rousseau D. (1985) - La stratigraphie des loess et formations fluviatiles d'Achenheim (Alsace): nouvelles données bioclimatiques et corrélations avec les séquences pléistocènes de la France du Nord-Ouest. Quaternaire, 22 (2), 125–132.

DOI : 10.3406/quate.1985.1536

Lawler D.M. (1993) - The measurement of river bank erosion and lateral channel change: A review. Earth Surface Processes and Landforms, 18 (9), 777–821.
DOI : 10.1002/esp.3290180905

Lea D.M., Legleiter C.J. (2016) - Refining measurements of lateral channel movement from image time series by quantifying spatial variations in registration error. Geomorphology, 258, 11–20.
DOI : 10.1016/j.geomorph.2016.01.009

Legleiter C.J. (2012) - Remote measurement of river morphology via fusion of LiDAR topography and spectrally based bathymetry: Measuring river morphology with LiDAR and spectral bathymetry. Earth Surface Processes and Landforms, 37 (5), 499–518.
DOI : 10.1002/esp.2262

Leopold L.B., Wolman M.G., Miller J.P. (1992) - Fluvial processes in geomorphology. Dover Publications, New York, 522 p.

Lespez L., Viel V., Rollet A.J., Delahaye D. (2015) - The anthropogenic nature of present-day low energy rivers in western France and implications for current restoration projects. Geomorphology, 251, 64–76.
DOI : 10.1016/j.geomorph.2015.05.015

Leypold D. (1995) - Mines et métallurgie du fer dans le massif vosgien de l'antiquité au XIXe siècle: l'exemple de la vallée de la Bruche. PhD Thesis. Université de Strasbourg, 1018 p.

Liébault F., Piégay H. (2001) - Assessment of channel changes due to long-term bedload supply decrease, Roubion River, France. Geomorphology, 36 (3), 167–186.
DOI : 10.1016/S0169-555X(00)00044-1

Liébault F., Piégay H. (2002) - Causes of 20th century channel narrowing in mountain and piedmont rivers of southeastern France. Earth Surface Processes and Landforms, 27 (4), 425–444.
DOI : 10.1002/esp.328

Liro M. (2015) - Estimation of the impact of the aerialphoto scale and the measurement scale on the error in digitization of a river bank. Zeitschrift für Geomorphologie, 59 (4), 443–453.
DOI : 10.1127/zfg/2014/0164

Lovric N., Tosic R. (2016) - Assessment of Bank Erosion, Accretion and Channel Shifting Using Remote Sensing and GIS: Case Study – Lower Course of the Bosna River. Quaestiones Geographicae, 35 (1), 81–92.
DOI : 10.1515/quageo-2016-0008

Magirl C.S., Webb R.H., Griffiths P.G. (2005) - Changes in the water surface profile of the Colorado River in Grand Canyon, Arizona, between 1923 and 2000. Water resources research, 41 (5).
DOI : 10.1029/2003WR002519

Maire G. (1966) - La Basse-Bruche : cône de piedmont et dynamique actuelle. PhD Thesis. Université de Strasbourg, Faculté de géographie et d'aménagement, 138 p.

Maire G. (1967) - La Basse-Bruche : quelques aspects de dynamique fluviale. Centre de géographie appliquée de Strasbourg, 55 p.

Maire G. (1985) - Etude hydro-géomorphologique de la Bruche : Détermination de secteurs homogènes. Centre de géographie appliquée de Strasbourg, 134 p.

Malavoi J.-R., Bravard J.-P. (2010) - Éléments d'hydromorphologie fluviale. Onema, 228 p.

Mandarino A., Maerker M., Firpo M. (2019) - Channel planform changes along the Scrivia River floodplain reach in northwest Italy from 1878 to 2016. Quaternary Research, 91 (2), 620–637.
DOI : 10.1017/qua.2018.67

Mann H.B. (1945) - Nonparametric Tests Against Trend. Econometrica, 13 (3), 245.
DOI : 10.2307/1907187

Marçal M., Brierley G., Lima R. (2017) - Using geomorphic understanding of catchment-scale process relationships to support the management of river futures: Macaé Basin, Brazil. Applied Geography, 84, 23–41.
DOI : 10.1016/j.apgeog.2017.04.008

Mariet A.-L. (2018) - Tracking past mining activity using trace metals, lead isotopes and compositional data analysis of a sediment core from Longemer Lake, Vosges Mountains, France. Journal of Paleolimnology, 14.
DOI : 10.1007/s10933-018-0029-9

Marston R.A., Bravard J.-P., Green T. (2003) - Impacts of reforestation and gravel mining on the Malnant River, Haute-Savoie, French Alps. Geomorphology, 55 (1–4), 65–74.
DOI : 10.1016/S0169-555X(03)00132-6

Millar R.G. (2000) - Influence of bank vegetation on alluvial channel patterns. Water Resources Research, 36 (4), 1109–1118.
DOI : 10.1029/1999WR900346

Millot G., Camez T., Wernert P. (1957) - Évolution des minéraux argileux dans les loess et les lehms d'Achenheim (Alsace). Sciences Géologiques, bulletins et mémoires, 10 (2), 17–19.
DOI : 10.3406/sgeol.1957.1163

Notebaert B., Verstraeten G. (2010) - Sensitivity of West and Central European river systems to environmental changes during the Holocene: A review. Earth-Science Reviews, 103 (3–4), 163–182.
DOI : 10.1016/j.earscirev.2010.09.009

Orr H.G., Large A.R.G., Newson M.D., Walsh C.L. (2008) - A predictive typology for characterising hydromorphology. Geomorphology, 100 (1–2), 32–40.
DOI : 10.1016/j.geomorph.2007.10.022

Payraudeau S., Galliot N., Liébault F., Auzet A.-V. (2010) - Incertitudes associées aux données géographiques pour la quantification des vitesses de migration des méandres-Application à la vallée de la Bruche. Revue Internationale de Géomatique, 20 (2), 221–243.
DOI : 10.3166/rig.20.221-243

Payraudeau S., Glatron S., Rozan A., Eleuterio J., Auzet A.-V., Weber C., Liébault F. (2008) - Inondation en espace péri-urbain: convoquer un éventail de disciplines pour analyser l'aléa et la vulnérabilité de la basse-Bruche (Alsace). In Actes Du Colloque «Vulnérabilités Sociétales, Risques et Environnement. Comprendre et Évaluer». Université Toulouse–le Mirail, 15 p.

Peeters A., Houbrechts G., Hallot E., Van Campenhout J., Gob F., Petit F. (2020) - Can coarse bedload pass through weirs? Geomorphology, 359, 107131.
DOI : 10.1016/j.geomorph.2020.107131

Petts G.E. (1984) - Impounded rivers: perspectives for ecological management. Wiley, 344 p.

Piégay H., Darby S.E., Mosselman E., Surian N. (2005) - A review of techniques available for delimiting the erodible river corridor: a sustainable approach to managing bank erosion. River Research and Applications, 21 (7), 773–789.
DOI : 10.1002/rra.881

Pohlert T. (2020) - trend: Non-Parametric Trend Tests and Change-

Point Detection. R package version 1.1.2.

Rinaldi M. (2003) - Recent channel adjustments in alluvial rivers of Tuscany, central Italy. Earth Surface Processes and Landforms, 28 (6), 587–608.
DOI : 10.1002/esp.464

Roux C., Alber A., Bertrand M., Vaudor L., Piégay H. (2015) - "FluvialCorridor": A new ArcGIS toolbox package for multiscale riverscape exploration. Geomorphology, 242, 29–37.
DOI : 10.1016/j.geomorph.2014.04.018

Salit F., Arnaud-Fassetta G., Zaharia L., Madelin M., Beltrando G. (2015) - The influence of river training on channel changes during the 20th century in the Lower Siret River (Romania). Géomorphologie : relief, processus, environnement, 21 (2), 175–188.
DOI : 10.4000/geomorphologie.11002

Schmitt L., Maire G., Nobelis P., Humbert J. (2007) - Quantitative morphodynamic typology of rivers: a methodological study based on the French Upper Rhine basin. Earth Surface Processes and Landforms, 32 (11), 1726–1746.
DOI : 10.1002/esp.1596

Schook D.M., Rathburn S.L., Friedman J.M., Wolf J.M. (2017) - A 184-year record of river meander migration from tree rings, aerial imagery, and cross sections. Geomorphology, 293, 227–239.
DOI : 10.1016/j.geomorph.2017.06.001

Schumm S.A. (1985) - Patterns of alluvial rivers. Annual Review of Earth and Planetary Sciences, 13 (1), 5–27.
DOI : 10.1146/annurev.ea.13.050185.000253

Simon A., Castro J., Rinaldi M. (2016) - Channel form and adjustment: characterization, measurement, interpretation and analysis. In Kondolf, G.M., Piégay, H. (Eds.): Tools in Fluvial Geomorphology. John Wiley & Sons, Ltd, Chichester, UK, 233–259.
DOI : 10.1002/9781118648551.ch11

Simon A., Rinaldi M. (2006) - Disturbance, stream incision, and channel evolution: The roles of excess transport capacity and boundary materials in controlling channel response. Geomorphology, 79 (3–4), 361–383.
DOI : 10.1016/j.geomorph.2006.06.037

Skupinski G., BinhTran D., Weber C. (2009) - Les images satellites Spot multi-dates et la métrique spatiale dans l'étude du changement urbain et suburbain – Le cas de la basse vallée de la Bruche (Bas-Rhin, France). Cybergeo, 439.
DOI : 10.4000/cybergeo.21995

Surian N., Mao L., Giacomin M., Ziliani L. (2009) - Morphological effects of different channel-forming discharges in a gravel-bed river. Earth Surface Processes and Landforms, 34 (8), 1093–1107.
DOI : 10.1002/esp.1798

Théobald N. (1955) - Les alluvions anciennes au sud de la Bruche et aux environs d'Obernai (Bas-Rhin). Sciences Géologiques, bulletins et mémoires, 8 (1), 83–104.
DOI : 10.3406/sgeol.1955.1148

Vogt H. (1992) - Le relief en Alsace: Etude géomorphologique du rebord sud-occidental du fossé rhénan. Librairie Oberlin, 239 p.

Volkmann H.-E., Müller R.-D. (1999) - Die Wehrmacht-Mythos und Realität: im Auftrag des Militärgeschichtlichen Forschungsamtes. Oldenbourg, München, 1318 p.

Werbylo K.L., Farnsworth J.M., Baasch D.M., Farrell P.D. (2017) - Investigating the accuracy of photointerpreted unvegetated channel widths in a braided river system: a Platte River case study. Geomorphology, 278, 163–170.
DOI : 10.1016/j.geomorph.2016.11.003

Winterbottom S.J. (2000) - Medium and short-term channel planform changes on the Rivers Tay and Tummel, Scotland. Geomorphology, 34 (3–4), 195–208.
DOI : 10.1016/S0169-555X(00)00007-6

Yao Z., Ta W., Jia X., Xiao J. (2011) - Bank erosion and accretion along the Ningxia–Inner Mongolia reaches of the Yellow River from 1958 to 2008. Geomorphology, 127 (1–2), 99–106.
DOI : 10.1016/j.geomorph.2010.12.010

Zar J.H. (2005) - Spearman Rank Correlation. In Armitage, P., Colton, T. (Eds.): Encyclopedia of Biostatistics. John Wiley & Sons, Ltd, Chichester, UK.
DOI : 10.1002/0470011815.b2a15150

Ziliani L., Surian N. (2012) - Evolutionary trajectory of channel morphology and controlling factors in a large gravel-bed river. Geomorphology, 173–174, 104–117.
DOI : 10.1016/j.geomorph.2012.06.001

Version française abrégée

Une majorité de rivières européennes a été largement affectée plus ou moins directement par divers aménagements et activités humaines (rectification, enrochements, canalisation, barrages, changement d'occupation du sol, extraction de granulats, etc.), menant à de profondes modifications de leur fonctionnement hydrogéomorphologique. L'étude géomorphologique de la trajectoire temporelle d'un cours d'eau consiste à reconstituer l'évolution de paramètres morphométriques du chenal, généralement par superposition de données diachroniques planimétriques (orthophotographies, cartes anciennes, etc.) et/ou verticales (levés historiques, modèles numériques de terrain, etc.). Ce type d'approche, largement éprouvée durant les dernières décennies, permet de caractériser le fonctionnement hydrogéomorphologique des cours d'eau, leur évolution, ainsi que leur sensibilité aux forçages hydro-climatiques et/ou anthropiques. La connaissance de la trajectoire hydrogéomorphologique d'un cours d'eau est aussi de plus en plus reconnu comme une base robuste permettant d'élaborer des stratégies de gestion - voire de restauration - durables des systèmes fluviaux.

La Basse-Bruche, sous-affluent du Rhin Supérieur, est une rivière alluviale de taille moyenne (superficie du bassin versant ~720 km²) qui conflue dans l'Ill aux portes de la ville de Strasbourg (fig. 1). Connue pour sa dynamique latérale active et ses inondations récurrentes (Maire, 1966 ; Payraudeau et al., 2010), elle a été largement impactée par de nombreuses activités humaines en particulier durant les périodes moderne et contemporaine (Klein, 2005 ; Skupinski et al., 2009), avec la construction du « Canal de la Bruche » à la fin du XVII^e siècle (Haettel et Haettel, 2012) et, depuis les années 1960, une urbanisation croissante (Skupinski, 2009). Présentant une concentration élevée de frayères à saumons (Salmo salar L.) et lamproies (Petromyzon marinus) (Gerlier et Roche, 1998), la Basse-Bruche constitue un système hydroécologique clé à l'échelle régionale qu'il convient de préserver, et dont les caractéristiques géomorphologiques et écologiques présentent un fort potentiel de restauration.

S'appuyant sur un large jeu de données diachroniques planimétriques et topographiques, l'objectif de cette étude est de reconstituer la trajectoire géomorphologique d'un tronçon de la Basse-Bruche de

6 km de long (fig. 1C). La période considérée couvre approximativement les 150 dernières années, de 1866 à 2015. Plus spécifiquement, l'étude vise à (i) quantifier précisément la mobilité latérale historique du tronçon d'étude, (ii) documenter l'évolution verticale du fond du lit et (iii) identifier les facteurs de contrôle des ajustements morphodynamiques enregistrés.

La base de données repose sur l'analyse de deux cartes anciennes, huit orthophotographies, deux MNT LiDAR (tab. 1) et un levé topographique ancien du fond du lit (fig. 5). Les incertitudes géométriques associées aux données planimétriques ont été finement évaluées, notamment sur la base des analyses de Jautzy et al. (2020).

Afin de quantifier précisément la mobilité latérale, le chenal actif a d'abord été digitalisé dans un système d'informations géographiques (SIG) pour chacune des données planimétriques disponibles. Puis, un indice de migration latérale (Aggregated Migration rate Index ; AMI) (fig. 3) a été spécialement conçu et appliqué sur les chenaux actifs digitalisés, pour permettre de documenter les ajustements latéraux de manière systématique, sur des tronçons élémentaires de 100 m.

L'analyse de l'évolution du profil longitudinal du fond du lit a d'abord nécessité le traitement des nuages de points des deux levés LiDAR diachroniques (2006, 2015). Le traitement a consisté à identifier au sein du nuage de points, ceux ayant été réfléchis à la surface de l'eau (fig. 4A) et à exclure ceux ayant été réfléchis sur des bancs alluviaux (fig. 4B). En moyennant les valeurs d'altitudes ainsi extraites, cela a permis d'obtenir deux profils longitudinaux diachroniques de la ligne d'eau. Les profils longitudinaux respectifs du fond du lit ont ensuite été obtenus en soustrayant la valeur du niveau d'eau mesurée à la station de jaugeage de Holtzheim, les jours respectifs des levés LiDAR. Les deux profils longitudinaux ainsi obtenus ont été convertis dans le même système de référence altimétrique que celui utilisé par le levé topographique ancien (EVRF2000).

Les résultats montrent que durant plus d'un siècle (de 1866 à 1978), la mobilité latérale de la Basse-Bruche était élevée (AMI moyen de 1,6 m/an) et distribuée de manière relativement homogène le long du tronçon d'étude. A l'inverse, de 1978 à 2015, la mobilité latérale moyenne a diminué de 50 % (LMI moyen de 0,8 m/an) et s'est concentrée dans la moitié aval du tronçon (sous-tronçons 18 à 38) (fig. 9). La construction d'un pipeline souterrain associée à de lourds aménagements du chenal entre 1965 et 1971 ont été identifiés comme la cause de cette altération du fonctionnement morphodynamique de la Basse-Bruche (sous-tronçons 8 à 13). La diminution de la largeur moyenne et l'augmentation de la sinuosité du tronçon témoignent également d'un ajustement géomorphologique encore en cours (fig. 8). La mobilité latérale du cours d'eau bien qu'actuellement réduite, est cependant toujours active, comme l'illustre les valeurs d'AMI des sous-tronçons 18, 28 et 35 entre 2011 et 2015 (8,1 ; 9,5 et 5,0 m/an, respectivement), ainsi que le différentiel des MNTs LiDAR 2006-2015 (fig. 12A).

L'évolution du profil longitudinal du fond du lit (fig. 10) révèle quant à lui une aggradation généralisée d'environ 0,6 m entre 1940 et 2006. Des hypothèses explicatives – qui peuvent se combiner - ont été formulées : les effets de la dernière phase de déforestation du massif Vosgien durant le XVIII^{e} siècle (Gebhardt et al., 2015) et d'éventuels arasements de seuils dans le bassin de la Bruche à l'amont du tronçon d'étude. De récentes et plus modestes aggradations (0,1-0,3 m) localisées aux alentours du pipeline et des ponts de Wolfisheim et Eckbolsheim, entre 2006 et 2015, ont également été enregistrées. Enfin, des analyses statistiques révèlent que le poids des facteurs hydro-climatiques (événements et/ou tendances) vis-à-vis des ajustements morphodynamiques n'est pas significatif.

Cette étude démontre que les ajustements géomorphologiques de la Basse-Bruche au cours des 150 dernières années ont été très largement contrôlés par les facteurs anthropiques. Au vu de la forte mobilité latérale mesurée entre la moitié du XIX^{e} et la moitié du XX^{e} siècle, il a aussi été mis en évidence que le potentiel de mobilité de ce secteur de la Basse-Bruche est très élevé. Ce dernier point devrait être pris en considération dans les futurs projets de gestion et de restauration de la dynamique latérale de la Basse-Bruche.